From Flash and Fire Points of Water Miscible Flammable Liquid Mixtures to a Novel Method of Membrane Characterization

By

Waseem Sabri

Supervisor
Boguslaw Kruczek, P.Eng., PhD

Thesis submitted to the University of Ottawa
in partial Fulfillment of the requirements for the
Master of Applied Science in Chemical Engineering

Department of Chemical & Biological Engineering
Faculty of Engineering
University of Ottawa

.

Table of Contents

List of Figures

List of Tables

Abstract

The National Fire Code and the National Building Code are two complimentary documents that outline the requirements for constructing or demolishing buildings and facilities in Canada. Part 4 of the fire code revolves around the storage, handling, building material requirements, leak detection systems, and piping requirements, among many other factors that must be considered for flammable and combustible materials. The codes consider a water-miscible flammable liquid (WMFL) mixture to be the same risk as a pure flammable liquid which intuitively is known to be incorrect. Diluting a flammable liquid with water will lower the fire safety risk by increasing the flash and fire point. Depending on the flash point, fire point, kinematic viscosity and boiling point, flammable liquids are placed into specific risk categories. Intuition itself is not enough to exclude WMFL mixtures from the pure flammable liquid category. Therefore a new category must be created by experimentally obtaining the flash point, fire point, kinematic viscosity and boiling point of WMFL mixtures. The results of this project allowed for quantification of the expected trends and might be used to justify changing the categorization of WMFL mixtures in the codes.

Improved gas separation membranes require developing new membrane materials, typically synthetic polymers. In turn, it requires their accurate characterization. Membrane characterization, i.e. obtaining the fundamental transport properties of the membrane material, is usually done using the time lag method in a constant volume system. The time-lag method allows the determination of the permeability, diffusivity and solubility in polymeric gas separation membranes from a single dynamic gas permeation experiment. The time lag method involves exposing a membrane that is originally degassed to a sudden increase in pressure upstream of the membrane. The rate of pressure increase in the downstream receiving volume is monitored, which produces a pressure rise curve which can be used to extract the membrane properties. For the complete characterization of glassy polymer membranes, multiple time lag experiments are required at varying pressures. A novel time-lag protocol is proposed based on a series of step changes in the feed pressure (steps up followed by steps down), equivalent to multiple time lag experiments. Unlike the classical time-lag protocol, the initial condition for the characterized membrane in the new protocol is a linear concentration profile within the membranes instead of a uniform, zero concentration across the membrane. Preliminary results in this project indicate the feasibility of the proposed new protocol.

Résumé

Le Code National de Prévention des Incendies et le Code National du Bâtiment sont deux documents complémentaires qui décrivent les exigences relatives à la construction ou à la démolition de bâtiments et d'installations au Canada. La partie 4 du code de prévention des incendies porte sur l'entreposage, la manutention, les exigences relatives aux matériaux de construction, les systèmes de détection des fuites et les exigences relatives à la tuyauterie, entre autres facteurs qui doivent être pris en compte pour les matières inflammables et combustibles. Les codes considèrent qu'un mélange liquide inflammable miscible à l'eau présente le même risque qu'un liquide inflammable pur. Ce qui, intuitivement, est incorrect. La dilution d'un liquide inflammable avec de l'eau diminue le risque d'incendie en augmentant le point d'éclair/de feu. En fonction du point d'éclair, du point de feu, de la viscosité cinématique et du point d'ébullition, les liquides inflammables sont classés dans des catégories de risque spécifiques. L'intuition seule ne suffit pas à exclure ces mélanges de la catégorie des liquides inflammables purs. Il faut donc créer une nouvelle catégorie en obtenant le point d'éclair, le point de feu, la viscosité cinématique et le point d'ébullition. Les résultats ont permis de quantifier les tendances attendues et pourraient être utilisés pour justifier la modification de la catégorisation de ces mélanges dans les codes.

L'amélioration des membranes de séparation des gaz nécessite le développement de nouveaux matériaux membranaires, généralement des polymères synthétiques. En retour, cela nécessite leur caractérisation précise. La caractérisation des membranes, c'est-à-dire la détermination des propriétés fondamentales de transport du matériau membranaire, est généralement obtenue par la méthode du décalage temporel dans un système à volume constant. La méthode du décalage temporel permet de déterminer la perméabilité, la diffusivité et la solubilité des membranes polymères de séparation des gaz à partir d'une seule expérience dynamique de perméation des gaz. La méthode consiste à exposer une membrane initialement dégazée à une augmentation soudaine de la pression en amont. Le taux d'augmentation de la pression dans le volume récepteur en aval est surveillé, ce qui produit une courbe d'augmentation de la pression qui peut être utilisée pour extraire les propriétés de la membrane. Pour la caractérisation complète des membranes polymères vitreuses, de multiples expériences de décalage dans le temps sont nécessaires à différentes pressions. Un nouveau protocole de décalage temporel est proposé, basé sur une série de changements progressifs de la pression d'alimentation (augmentation suivie d'une diminution), équivalant à plusieurs expériences de décalage temporel. Contrairement au protocole classique de décalage temporel, la condition initiale pour la membrane caractérisée dans le nouveau protocole est un profil de concentration linéaire à l'intérieur des membranes au lieu d'une concentration nulle uniforme à travers la membrane. Les résultats préliminaires de ce projet indiquent la faisabilité du nouveau protocole proposé.

Statement of Contributions

I hereby declare that this work has not been submitted or accepted for any other degree. Dr. Boguslaw Kruczek and Dr. Hassan Rokib supervised the research performed in this thesis.

Chapter 2: Testing and Data Analysis of Water Miscible Flammable Liquid Mixtures

The laboratory was located at the National Research Council (NRC) and all provided equipment is owned by the NRC. This project was first started by Dr. Rokib Hassan, who completed the literature review for the project. My work in the lab and training was directly supervised by Benjamin Jones, MASc. This chapter was reviewed by Dr. Rokib Hassan, Dr. Uttam Das and Dr. Boguslaw Kruczek.

Chapter 3: Novel Methods of Membrane Characterization using Steady State Step Changes

The laboratory was located at the University of Ottawa and the experimental set up is owned by Dr. Boguslaw Kruczek. The membrane set-up was first created by Dr.Kruczek, but significant changes were made by Peter Jr Leszczynski. The experimental protocol was modified over the years, the latest protocol was provided by Peter Jr Leszczynski. All the membranes were created by Peter Jr Leszczynski. Zheng Cao greatly assisted with the experiments in the lab.

Acknowledgements

I'd like to thank Dr. Boguslaw Kruczek - a fantastic professor and mentor. You helped me face adversity and provided me with the confidence throughout my graduate studies. I am forever grateful for your kind words and advice in regards to my studies and to my future endeavours. I'd also like to thank Peter Leszczynski and Zheng Cao – two friends and colleagues that assisted me throughout my studies.

Thank you to the National Research Council and the University of Ottawa for providing me with this opportunity.

Chapter 1. Thesis Objectives and Introduction

1.1 Overview of the Thesis

This thesis consists of four chapters – the first chapter is this introduction, the second chapter is the flash/fire point determination of water-miscible flammable liquid mixtures, the third chapter is a novel method of membrane characterization, and the fourth is the overall conclusions and recommendations.

My first thesis project, chapter two of this thesis, was provided by the National Research Council (NRC) of Canada. The goal of this project was to determine the flash and fire point of various water-miscible flammable liquid mixtures (WMFLs), along with boiling point and kinematic viscosity. The objective was to reduce the stringent regulations placed on WMFL storage and handling. As of now, WMFLs are considered to be just as hazardous as pure flammable liquids, which places a strain on industries such as the windshield washer fluid industry, alcoholic beverage industry, etc. After one year of working on this project, funding was not renewed due to an internal NRC issue. As a result, I obtained a second project from Dr. Kruczek, to supplement the NRC project.

The second thesis project is related to membrane characterization. The project revolved around performing a novel time-lag protocol based on a series of step changes in the feed pressure (steps up followed by steps down), equivalent to multiple time lag experiments.

1.2 Flammable and Combustible Liquids

Liquids that produce ignitable vapours can be classified as either flammable or combustible. Flammable liquids give off enough vapour at normal working temperatures to catch fire. A combustible liquid does not produce enough vapor at normal working temperatures to catch fire. The official definition of a flammable/combustible liquid is as follows: a flammable liquid has a flash point under 37.8° C (100° F), and a combustible liquid has a flash point between 37.8 to 93.3° C (100 to 200° F)[1].

A material's tendency to be flammable is characterized by the flash and fire point, which are defined as the following [1]:

a) Flash Point: the lowest temperature at which vapours above a liquid will ignite when exposed to an ignition source.
b) Fire Point: the lowest temperature at which the vapours evolve above a liquid at a sufficient rate to support ongoing combustion.

The lower explosive limit (LEL) is another important characteristic of a flammable/combustible liquid. It is defined as: The lowest concentration of vapour in the air that will burn or explode upon contact with a source of ignition [1].

1.2.1 Flash and Fire Point Determination

The flash point is determined experimentally by heating a vessel containing the flammable/combustible liquid and monitoring the temperature using either a thermometer or thermocouple [2]. A flame is brought near the surface of the liquid at regular intervals [2]. If a flash occurs in the vessel, it indicates that the temperature of the tested liquid has reached (or exceeded) the flash point [2].

The flash and fire point of a sample can be determined experimentally using a closed or open cup flash point tester. The difference between the two being that with an open cup tester, the sample is exposed to the atmosphere, while a closed cup tester is not. Therefore, the closed cup tester provides the equilibrium flash/fire point since the vapors cannot escape. In the closed cup tester, the equilibrium exists between the liquid, vapor and air. In the open cup tester, the vapor produced by the liquid will constantly escape, and it will never reach equilibrium. The flash point of a mixture containing a single flammable compound can be found mathematically using equation 1.0 below [2].

$$LFL \cdot P = \gamma_i x_i P_{i,FP}^{SAT} \qquad 1.0$$

Equation 1.0 is essentially modified Raoult's Law, with the vapor fraction term being replaced with the LFL. The variable γ_i is the activity coefficient of species i, x_i is the molar fraction of the liquid and $P_{i,FP}^{SAT}$ is the saturation pressure of species i at flash point temperature [2]. The difficulty of using this method is obtaining confident activity coefficients. Nevertheless, experimentally determined flash and fire points using either a closed cup or open cup tester are required by the National Research Council to update the codes.

1.3 Gas Separation Membranes

A membrane is a barrier that separates two phases and allows for the transport of material from one phase to another while inhibiting the transport of other materials. This is the basis for membrane separation processes – one or more substances of interest can pass through the membrane while the transport of remaining substances partly or entirely restricted. Membranes can be broken up into biological membranes and synthetic membranes, which can further be broken up by the material of construction. Examples of synthetic membranes are: polymeric, ceramic and liquid membranes.

A simple diagram of a membrane separation process is shown below in Figure 1.1. The feed enters the membrane module and is split into a permeate (the portion that passes through the membrane) and a retentate stream.

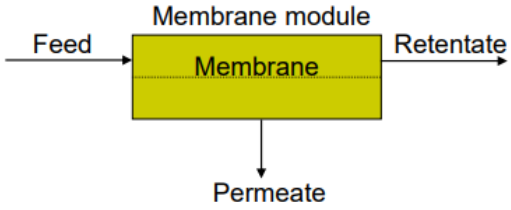

Figure 1-1: Simple membrane system [3]

Membranes are classified as either porous or non-porous (dense) membranes. The primary mechanism of transport through porous membranes depends on the membrane pore size relative to the size of the permeating molecules. For non-porous membranes, the mechanism of transport is "solution-diffusion", where the particles are adsorbed onto the membrane surface and diffuse through the material. Figure 2 shown below, summarizes the transport of particles through membranes with different pore sizes. The first three membranes (a, b and c) are porous membranes of varying pore sizes, while the fourth membrane (d) is a dense membrane which does not have permanent pores across the membrane. Bulk flow is a dominating mechanism when the pore size is much larger than the mean free path of permeating gases (Figure 2a). All permeating molecules move then with the same velocity, and no separation is

possible. When the mean free path of permeating molecules is smaller than the membrane's pore size (Figure 2b), the dominating mechanism is Knudsen diffusion, in which a limited selectivity is possible based on the molecular weight of the permeating gases. When the pore size becomes comparable to the permeating species, the dominating mechanism is molecular sieving, which can provide very high selectivities. Most currently used gas separation membranes have a dense structure of the selective layer (Figure 2d) and rely on the solution-diffusion mechanism.

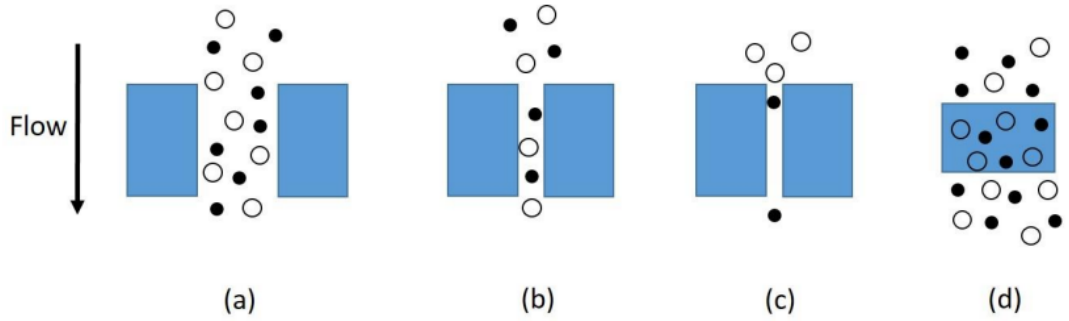

Figure 1-2: Summary of transport methods, a) Bulk flow through pores, b) Knudsen diffusion, c) molecular sieving, d) solution diffusion through dense membranes [4].

1.3.1 Membrane Characterization

Membrane characterization means obtaining the properties of the membrane material. Examples of physical properties of membrane materials are density, porosity and tensile strength. Examples of the chemical properties of membrane materials are composition, crosslinking density and surface charge. The most important characteristics of a membrane in the context of gas separation processes are solubility, diffusivity and permeability of permeating species, which are transport properties.

The most common method of obtaining the transport properties of membrane material is through the time-lag method in a constant volume system, originated by the work of Daynes [5]. This method is also used for studying gas permeation through industrial film applications, such as food packing and hollow membranes [6]. In the time-lag method, the gas of interest passes through the membrane as a result of the instantaneous pressure differential between the feed and permeate side of the membrane. The gas accumulates on the low-pressure permeate side and is monitored with a pressure transmitter [5]. At a steady state, the gas flux through the membrane and, thus, the rate of pressure increase become constant [5]. It is important to note that this is a pseudo-steady state because as the pressure increases on the permeate side, the driving force decreases. This pressure rise is slight for barrier materials with low permeation rates and is assumed to have no effect on the driving force. Figure 1-3 below outlines a typical pressure profile of a time-lag experiment performed in a constant volume system.

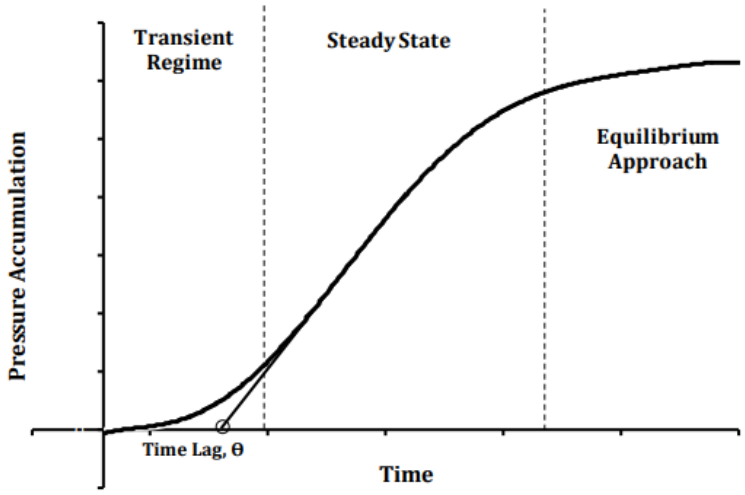

Figure 1-3: Typical pressure response in a constant volume system [7].

The transient region exists when the experiment is initiated, and permeation begins, followed by a pseudo-steady state and, eventually, once the pressure in the downstream volume nears the feed pressure, an equilibrium approach. The time lag is indicated by the x-intercept of the steady state portion of the pressure profile. The time lag and the slope of the steady state portion are used to extract the transport properties, which will be further discussed in Chapter 3.

References

[1] Flammable and combustible liquids, Health Canada, 2006, www.ccohs.ca

[2] Flash and fire point determination of binary mixtures of alcohols, ketones and water, P.J. Martínez, E. Rus and J.M. Compaña

[3] B. Dr. Kruczek, CHG 8198: Membrane Gas Separation Processes, 2021.

[4] Wikipedia, Mechanisms of Transport in Membranes, (2016). https://en.wikipedia.org/wiki/Membrane_gas_separation#/media/File:Mechanisms_of_transport_i n_membranes.jpg.

[5] N. Al-Qasas, J. Thibault, B. Kruczek, Analysis of gas transport in laminated semi-infinite solid: Novel method for complete membrane characterization during highly transient state, J Memb Sci. 460 (2014) 25-33.

[6] N. Al-Qasas, J. Thibault, B. Kruczek, A new characterization method of membranes with nonlinearsorption isotherm systems based on continuous upstream and downstream time-lag measurements, J Memb Sci. 542 (2017) 91–101.

[7] Mukhtar Al-Ismaily, A Novel Method of Characterizing Polymer Membranes Using Upstream Gas Permeation Tests, 2011

Chapter 2. Testing and Data Analysis of Water Miscible Flammable Liquid Mixtures

Abstract

Water miscible flammable liquids (WMFLs) are organic polar liquids which are fully miscible in water and used in a variety of commercial products. Due to the fact that the WMFLs present in commercial products are mixed with water, they possess lower fire hazards compared to pure flammable liquids. However, they are still considered hazardous. The National Fire Code (NFC) considers these mixtures to be pure flammable liquids which places a burden on the windshield washer fluid industry, alcoholic beverage industry, among other flammable liquid manufacturers. The Standing Committee on Hazardous Materials and Activities struck a Task Group (TG) – the TG agreed to create a research project to address the WMFL issue.

The physical properties of interest for the TG included kinematic viscosity, boiling point, flash point and fire point. Five WMFLs were studied in this report, along with five commercial products that contain some of these WMFLs. The WMFLs included Methanol, Ethanol, 2-Propanol, Acetone and Acetic Acid. The commercial products included Reflex Windshield Washer Fluid (-49 ^{o}C), Certified Windshield Washer Fluid (-35 ^{o}C), Certified Plumbing Antifreeze (-50 ^{o}C), Equate Rubbing Alcohol and Allen's Double Strength Cleaning Vinegar.

The kinematic viscosity was determined using the LOVIS 2000 ME & DMA dynamic viscometer and density meter. The boiling point was obtained using the PILODIST 1120C boiling instrument. The flash and fire points were obtained using the Koehler open-cup flash and fire point tester.

Each WMFL was mixed with water to obtain the concentrations of interest, which were decided through collaborations between the National Research Council (NRC) and the client. The kinematic viscosity, boiling point, flash point and fire point of each concentration were tested in triplicate for statistical significance. Each commercial product was also tested in triplicate, which led to a total of 540 samples.

It was found that the flash and fire point of aqueous solutions of WMFLs had lower flash and fire points, which results in a lower fire safety risk. Therefore, these substances should be put into a new category with less stringent storage and handling regulations.

2.1 Introduction

2.1.1 Water Miscible Flammable Liquids

Water-miscible flammable liquids (WMFLs) are organic polar liquids that are fully miscible in water and used in a variety of commercial products such as windshield washer fluids, alcoholic beverages, rubbing alcohols, air fresheners, hair sprays and pharmaceutical products [1]. The concentration of these WMFLs depends on the application – for example, windshield washer fluids usually contain methanol to lower the freezing point of the solution, and the specific methanol content will be higher for lower temperature conditions [1]. Since WMFLs are mixed with water in most commercial products, they possess lower fire hazards compared to pure flammable liquids – this is because the dilution effect of the water reduces the liquid's ability to sustain combustion [1,2]. As a result, the flash and fire point of most commercial products are higher than their pure flammable liquid counterparts [1]. Although WMFLs mixed with water are considered to have lower risks than pure flammable substances, recent studies suggest they can pose significant fire hazards and, therefore, must be investigated [1].

2.1.2 WMFLs and the National Fire Code

The National Research Council (NRC) states the following: "The National Fire Code of Canada 2015 (NFC), published by the National Research Council and developed by the Canadian Commission on Building and Fire Codes (CCBFC), sets out the technical provisions regulating activities related to the construction, use or demolition of buildings and facilities, the condition of specific elements of buildings and facilities, and the design or construction of specific elements of facilities related to certain hazards as well as the protection measures for the current or intended use of buildings" [2,3]. Currently, the NFC does not consider the dilution effect of water in WMFL – water mixtures and treats them as pure flammable substances; this places an unnecessary burden on the construction industry [1].

The CCBFC approved a task to address the Water-miscible flammable liquids (WMFLs) issue. The Standing Committee on Hazardous Materials and Activities gave this task a high priority and struck a Task Group (TG). The scope of this task is to determine the appropriate level of protection for WMFLs in all occupancies, including industries. The TG agreed to create a research project for evaluating the detailed fire hazards of WMFLs and to provide results on the chemical and physical properties of WMFLs. These results will help classify WMFLs and assess necessary protection measures [1]. I, Waseem Sabri from the University of Ottawa, was tasked by the NRC to assist in the testing and analyzing of these WMFLs, among other tasks.

2.1.3 Project Scope

One of the objectives of the contract was to determine the kinematic viscosity (cSt), boiling point (°C), and open-cup flash and fire points (°C) of the first 5 water-miscible flammable liquids (WMFLs; blue) out of the listed 20 WMFLs (Table 2-1) [1].

Table 2-1: List of 20 WMFLs

No.	WMFLs	Project Phase
1.	Methanol	project Phase 2 (2020-2021)
2.	Ethanol	

3.	2-Propanol (Isopropyl alcohol)	
4.	Acetone	
5.	Acetic acid	
6.	Methanol:Ethanol mixture	-
7.	Methanol:2-Propanol mixture	
8.	1-Propanol (*n*-Propyl alcohol)	
9.	Isobutanol (Isobutyl alcohol)	
10.	*tert*-Butanol (*tert*-Butyl alcohol)	
11.	Allyl alcohol	
12.	2-Isopropoxyethanol (Isopropylglycol)	
13.	Acetaldehyde	
14.	2,3-Butanedione (Butane-2,3-dione)	
15.	1,4-Dioxane	
16.	Tetrahydrofuran (THF)	
17.	Morpholine	
18.	Cyclohexylamine	
19.	*N,N*-Dimethylformamide (DMF)	
20.	Acetonitrile	

Table 2-2 shows the selected 5 WMFLs and their respective commercial product brands. The chemical content of Reflex Windshield Washer Fluid, -49 °C [4], Certified Windshield Washer Fluid, -35 °C [5], and Certified Plumbing Antifreeze, -50 °C [6] were obtained from their respective up-to-date safety data sheets (SDSs) as collected from the Canadian Tire store. The chemical contents of Equate Rubbing Alcohol and Allen's Double Strength Cleaning Vinegar were found on their labels as 70% vol. of 2-Propanol (Isopropyl alcohol) [7] and 10% vol. of Acetic acid [8], respectively.

Table 2-2: List of commercial products tested with corresponding to 5 WMFLs

No.	WMFLs	Commercial products[†]	Chemical contents (% vol.)
1.	Methanol	Reflex Windshield Washer Fluid, -49 °C	Methanol (30–60%) Ethylene glycol (0.5–1.5%)
		Certified Windshield Washer Fluid, -35 °C	Methanol (30–60%)
2.	Ethanol	Certified Plumbing Antifreeze, -50 °C	Ethanol (10–30%) 1,2-Propylene glycol (1–5%)
3.	2-Propanol (Isopropyl alcohol)	Equate Rubbing Alcohol	2-Propanol (70%)
4.	Acetone[‡]	-	-
5.	Acetic acid	Allen's Double Strength Cleaning Vinegar	Acetic acid (10%)

[†] Images of selected commercial product brands are shown in Figure 2-1

[‡] No commercial product was found containing Acetone-Water mixture except 100% Acetone. Hence, no test was performed on Acetone containing commercial products as per the Working Group (WG) recommendation

Reflex Windshield Washer Fluid, -49 °C

Certified Windshield Washer Fluid, -35 °C

Certified Plumbing Antifreeze, -50 °C

Equate Rubbing Alcohol

Allen's Double Strength Cleaning Vinegar

Figure 2-1: Images of the commercial products tested in project Phase 2

Table 2-3 provides a detailed list of a sampling of each of the selected 5 WMFLs [1]. The working group recommended these concentrations for testing. Two additional Methanol concentrations (40% and 50%) were also tested (blue).

Table 2-3: Sampling details of selected 5 WMFLs

No.	Samples	Recommended % vol.	Tested % vol.		Sample no.
1.	Methanol	90	90	✓	10 samples
		80	80	✓	
		70	70	✓	
		60	60	✓	
		-	50	✓	
		-	40	✓	
		30	30	✓	

		20	20	✓	
		10	10	✓	
		5	5	✓	
2.	Ethanol	90	90	✓	10 samples
		70	70	✓	
		60	60	✓	
		50	50	✓	
		40	40	✓	
		30	30	✓	
		20	20	✓	
		15	15	✓	
		10	10	✓	
		5	5	✓	
3.	2-Propanol	90	90	✓	11 samples
		80	80	✓	
		70	70	✓	
		60	60	✓	
		50	50	✓	
		40	40	✓	
		30	30	✓	
		20	20	✓	
		10	10	✓	
		5	5	✓	
		2	2	✓	
4.	Acetone	20	20	✓	5 samples
		15	15	✓	
		10	10	✓	
		5	5	✓	
		3	3	✓	
5.	Acetic acid	95	95	✓	4 samples
		90	90	✓	
		80	80	✓	
		75	75	✓	
4 tests (boiling point, kinematic viscosity, flash point and fire point) and 3 replicates of each sample					(40x4x3) = **480** samples
5 commercial products					(5x4x3) = **60** samples
				Total (480+60)	**540** samples

2.2 Experimental Procedure

The following instruments (Figure 2-2) were used to measure the kinematic viscosity (cSt), boiling point (°C), and open-cup flash and fire points (°C) of selected 5 WMFLs in project Phase 2.

Lovis 2000 ME & DMA™ M

PILODIST 1120 CC

Koehler K15601 Open-Cup Flash and Fire Point Tester

Figure 2-2: List of instruments

Table 2-4 summarizes the measurement error of each instrument. A 200±5 mL sample was prepared for each WMFL-Water mixture (Table 2-3).

Table 2-4: Measurement error associated with the instrument

Instrument	Measurement	Measurement error
Lovis 2000 ME & DMA™ M	Kinematic Viscosity	±0.001 cSt
PILODIST 1120 CC	Boiling Point	±0.01 °C
Koehler K15601 Open-Cup Flash and Fire Point Tester	Flash and Fire Point	±1 °C

The Lovis 2000 ME & DMA viscometer was calibrated using pure distilled water and pure methanol. The PILODIST 1120 CC boiling point tester was calibrated using only distilled water. The Koehler open-cup flash point tester is a fully manual piece of equipment, i.e., the movement of the pilot flame was done by hand, and the flash/fire point was obtained by visual inspection (not electronically). Therefore calibrations were not needed. To abide by the ASTM D1310 standard, the temperature of the solutions was increased at a rate of about 1°C per minute. The aforementioned heating rate was obtained by controlling the electric heater to approximately 30% power, using distilled water and adjusting slightly depending on the solvent.

The following essential lab equipment was used to create the samples:

A. Volumetric flasks of varying volume
B. Graduated cylinders of varying volume
C. Chemical squeeze bottles

A B C

Figure 2-3: Summary of equipment used to create samples

For the pre-determined mixtures, the chemical of interest was first poured into the spray bottle shown above in Figure 2-3. Distilled water was poured into a separate squeeze bottle. To reduce the chance of contamination, each chemical had its dedicated squeeze bottle, which was rinsed with each respective chemical prior to use. The squeeze bottle was then used to fill a graduated cylinder to the volume of interest, which was then carefully poured into the volumetric flask. The remainder of the volumetric flask was filled using distilled water to the measured mark of the volumetric flask. If the chemical was in high concentration (>50%), distilled water was measured in the graduated cylinder, and the flask was filled to the measured mark. The error associated with creating the mixtures was calculated to be ±0.5 (% vol.).

2.2.1 Boiling Point Determination

To obtain the boiling points, 100 mL samples were prepared following the procedure stated prior. These samples were transferred into a PILODIST 60 mL measuring vessel which was then used to fill the round bottom flask that was placed inside the instrument. Three boiling chips were added to each sample prior to testing to promote nucleation and prevent bumping. The heating rates were kept relatively constant throughout the testing. The equilibrium boiling point was determined at the temperature at which the drop rate from the condenser was 1.5 drops per second and held constant for one minute. This test was repeated in triplicate for each sample.

2.2.2 Kinematic Viscosity Determination

Density and dynamic viscosity were determined using the Lovis 2000 ME Microviscometer, which was connected to DMA 4100M density meter. Using the density and dynamic viscosity, the kinematic viscosity was calculated. All densities and dynamic viscosities were reported at 37.8 ^{o}C. The take-off angle of the viscometer was set to 40^{o}. This angle was recommended by the Anton-Paar technician to reduce the chance of equipment malfunction. Samples were transferred to appropriate vials and performed in triplicate. The presence of bubbles inside the small vials could result in viscometer malfunction, where the capillary would need to be removed, cleaned and inserted back into the instrument. To mitigate this, each vial was decanted and left to sit to remove all bubbles. Silicon caps were placed on top of each vial to reduce volatile chemical evaporation. Once the automatic sampler was filled with vials, a simple press of a button allowed the instrument to cycle through each vial and obtain kinematic viscosity and density.

2.2.3 Flash and Fire Point Determination

The open cup flash and fire point were obtained following the ASTM D1310 standard. Firstly, 100 mL samples were prepared and chilled in the lab refrigerator (if the anticipated flash-point was below the

ambient temperature). A recirculator was also connected to the instrument to cool samples down to -10 °C if required. The sample was then transferred to the Koehler flash-point cup and placed inside the stainless steel cup holder. The level of the solution is an important parameter and needs to be consistent across all trials. A dedicated levelling tool provided by Koehler is used to fill the cup to the appropriate level. Once the sample temperature was about 10 °C below the anticipated flash point (closed cup values from the literature were used as the anticipated values), the heating element was engaged, and the temperature was monitored to ensure a heating rate of about 1 °C per minute. The pilot flame was then passed over the cup once every minute to observe a flash/fire point. Once the trial was completed, the heating element was turned off, and the recirculator was turned on. The fresh solution was added to the cup after each trial and topped off during the experiment if necessary.

2.3 Experimental Results

All raw data tables can be found in Appendix A.

2.3.1 Boiling Points

Boiling Point of Methanol

The boiling point of methanol at varying concentrations can be seen in Figure 2-4. This figure shows a gradual decrease in boiling points with increasing methanol concentrations. The measured boiling point of the Reflex Windshield Washer Fluid, -49 °C corresponds to 50% Methanol concentration. It should be noted that the Reflex Windshield Washer Fluid up-to-date SDS reported Methanol concentration was 30–60% in addition to 0.5–1.5% Ethylene glycol concentration [4]. The measured boiling point of the Certified Windshield Washer Fluid, -35 °C, corresponds to 40% methanol concentration. It should also be noted that the Certified Windshield Washer Fluid up-to-date SDS reported methanol concentration was 30–60% [5].

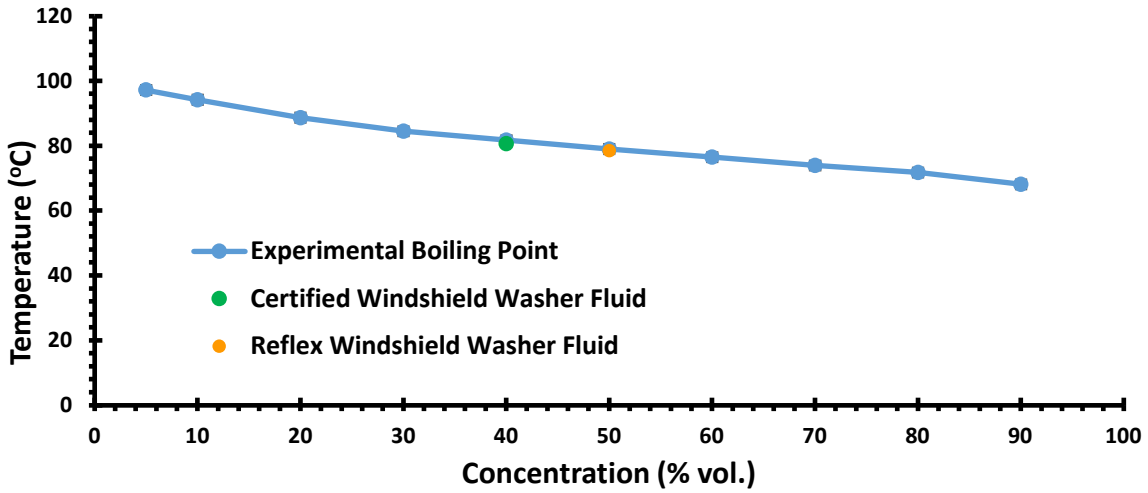

Figure 2-4: Boiling points of methanol-water mixture as a function of methanol concentration. The boiling points of two commercial products are also plotted.

Boiling Point of Ethanol

The boiling point of ethanol at varying concentrations can be seen in Figure 2-5. This figure shows a decrease in boiling points with increasing ethanol concentrations. The measured boiling point of the Certified Plumbing Antifreeze, -50 °C, corresponds to 40% ethanol concentration. It should be noted that the Certified Plumbing Antifreeze up-to-date SDS reported ethanol concentration was 10–30% in addition to 1–5% 1,2propylene glycol concentration [6].

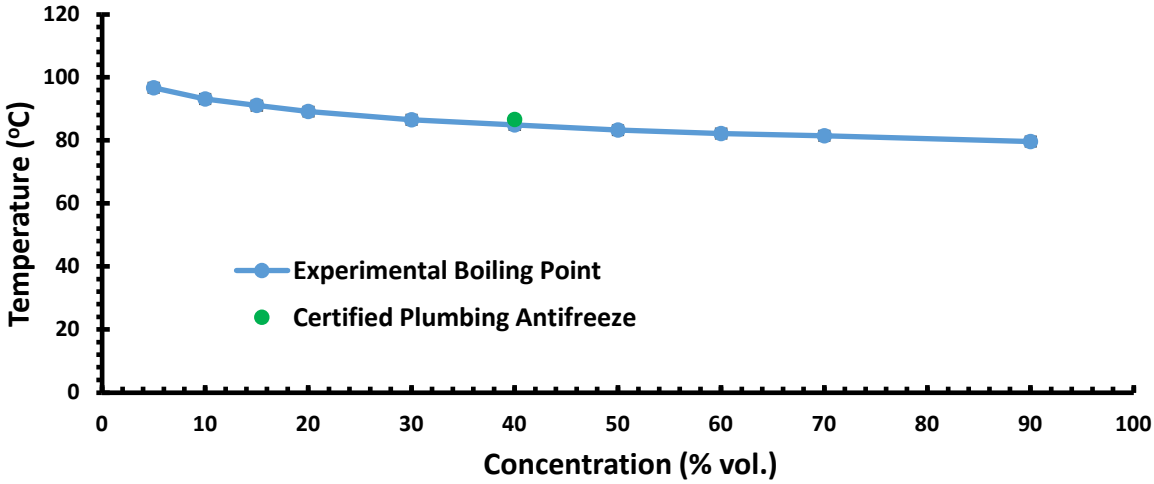

Figure 2-5: Boiling points of ethanol-water mixture as a function of ethanol concentration. The boiling point of a commercial product is also plotted.

Boiling Point of 2-Propanol

The boiling point of 2-propanol at varying concentrations can be seen in Figure 2-6. This figure shows a decrease in boiling points with increasing 2-propanol concentrations. The measured boiling point of the Equate Rubbing Alcohol corresponds to 70% 2-Propanol concentration. It should be noted that the Equate Rubbing Alcohol label reported a 2-propanol concentration of 70% [7].

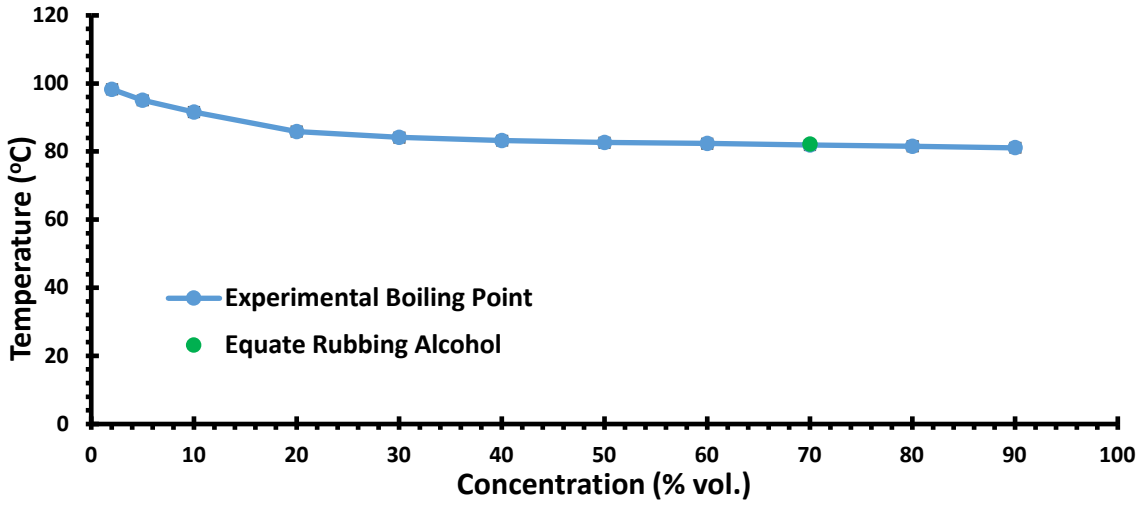

Figure 2-6: Boiling points of 2-propanol-water mixtures as a function of 2-propanol concentration. The boiling point of a commercial product is also plotted.

Boiling Point of Acetone

The boiling point of acetone at varying concentrations can be seen in Figure 2-7. This figure shows a decrease in boiling points with increasing acetone concentrations. It should be noted that no commercial products were found containing acetone-water mixture except 100% acetone. Therefore, no test was performed on acetone containing commercial products as per the WG recommendation.

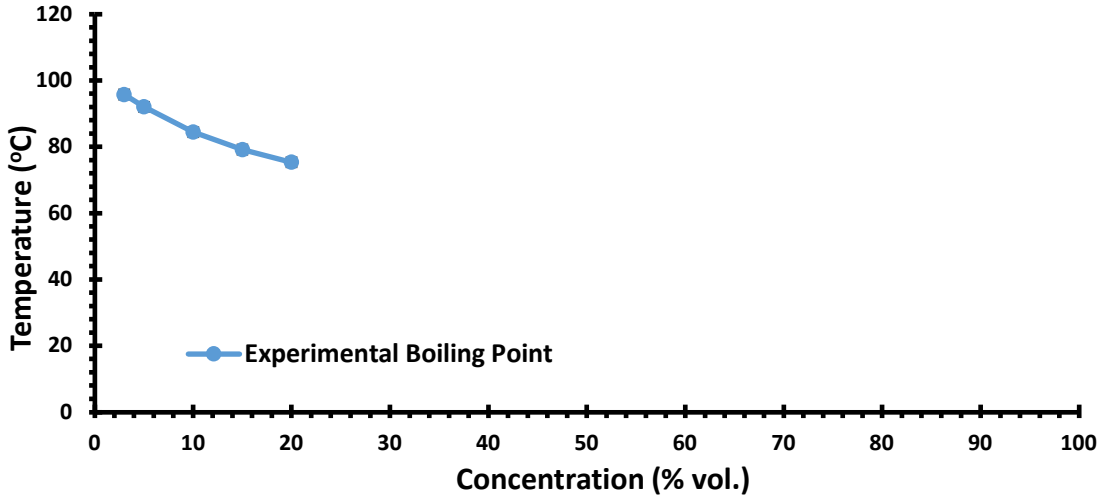

Figure 2-7: Boiling point of acetone-water mixture as a function of acetone concentration.

Boiling Point of Acetic Acid

The boiling point of acetic acid at varying concentrations can be seen in Figure 2-8. This figure shows an increase in boiling points with increasing acetic acid concentrations (Table 14). The measured boiling point of Allen's Double Strength Cleaning Vinegar corresponds to 10% acetic acid concentration (Table 14). It should be noted that Allen's Double Strength Cleaning Vinegar label reported an acetic acid concentration of 10% [8]. It should also be noted that the WG did not recommend any test for 10% acetic acid concentration (Table 3). Hence, no experimental boiling point of 10% acetic acid concentration was available to compare with Allen's Double Strength Cleaning Vinegar.

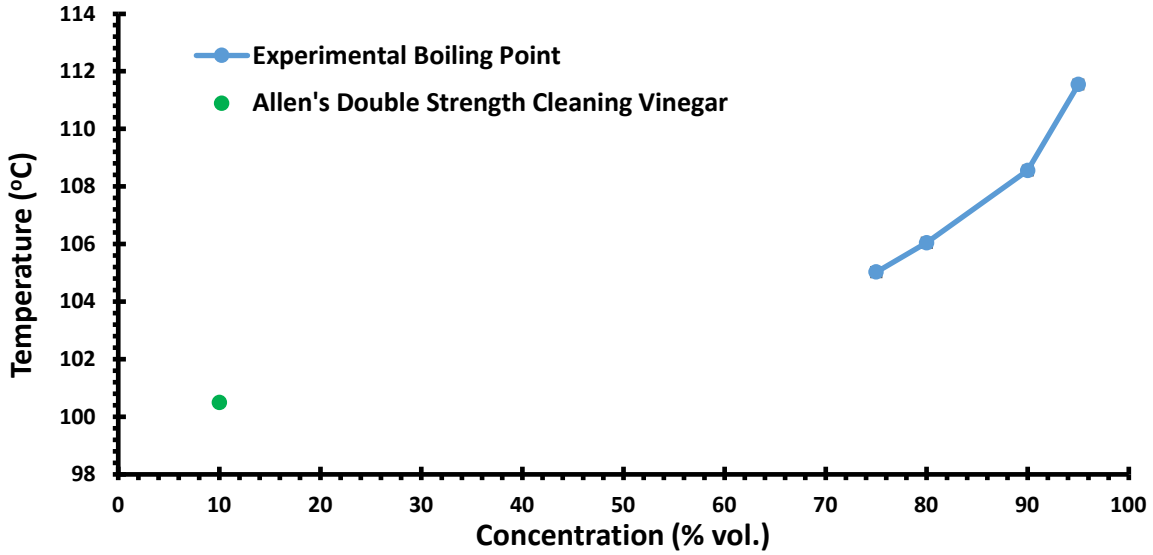

Figure 2-8: Boiling points of acetic acid-water mixture as a function of acetic acid concentration. The boiling point of a commercial product is also plotted.

2.3.2 Kinematic Viscosities

Kinematic Viscosity of Methanol

The kinematic viscosity of methanol at varying concentrations can be seen in Figure 2-9. This figure shows an initial increase in kinematic viscosities with increasing aethanol concentrations up to 50%. Later above 50%, this figure shows a decrease in kinematic viscosities with increasing nethanol concentrations up to 90%. The measured kinematic viscosity of the Reflex Windshield Washer Fluid, -49 °C, corresponds to 50% methanol concentration, whereas the measured kinematic viscosity of the Certified Windshield Washer Fluid, -35 °C corresponds to 40% methanol concentration.

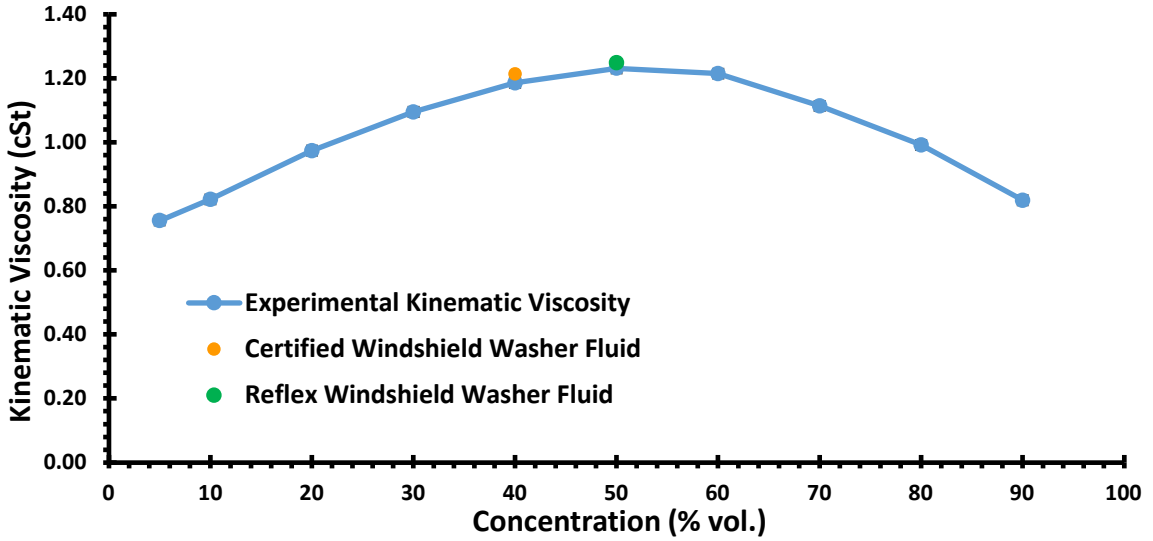

Figure 2-9: Kinematic viscosities of Methanol-Water mixture as a function of methanol concentration. Kinematic viscosity of two commercial products are also plotted.

Kinematic Viscosity of Ethanol

The kinematic viscosity of ethanol at varying concentrations can be seen in Figure 2-10. This figure shows an initial increase in kinematic viscosities with increasing ethanol concentrations up to 60%. Later above 60%, this figure shows a decrease in kinematic viscosities with increasing ethanol concentrations up to 90%. The measured kinematic viscosity of the Certified Plumbing Antifreeze, -50 °C, corresponds to 40% ethanol concentration.

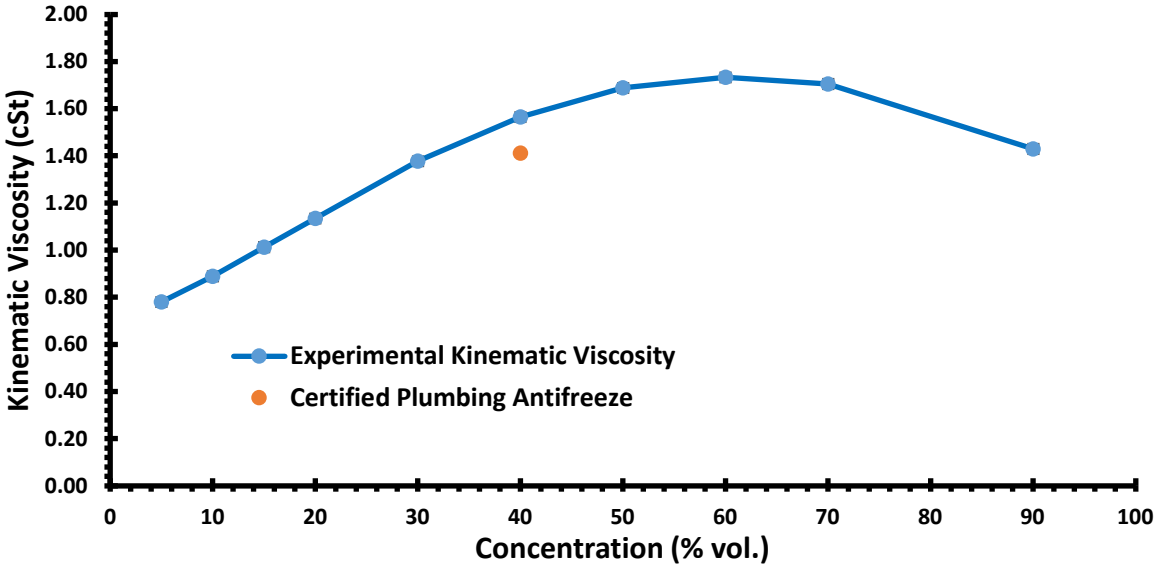

Figure 2-10: Kinematic viscosities of ethanol-water mixture as a function of ethanol concentration. Kinematic viscosity of a commercial product is also plotted.

Kinematic Viscosity of 2-Propanol

The kinematic viscosity of 2-propanol at varying concentrations can be seen in Figure 2-11. This figure shows an initial increase in kinematic viscosities with increasing 2-propanol concentrations up to 70%. Later above 70%, this figure shows a decrease in kinematic viscosities with increasing 2-propanol concentrations up to 90%. The measured kinematic viscosity of the Equate Rubbing Alcohol corresponds to 70% 2-propanol concentration.

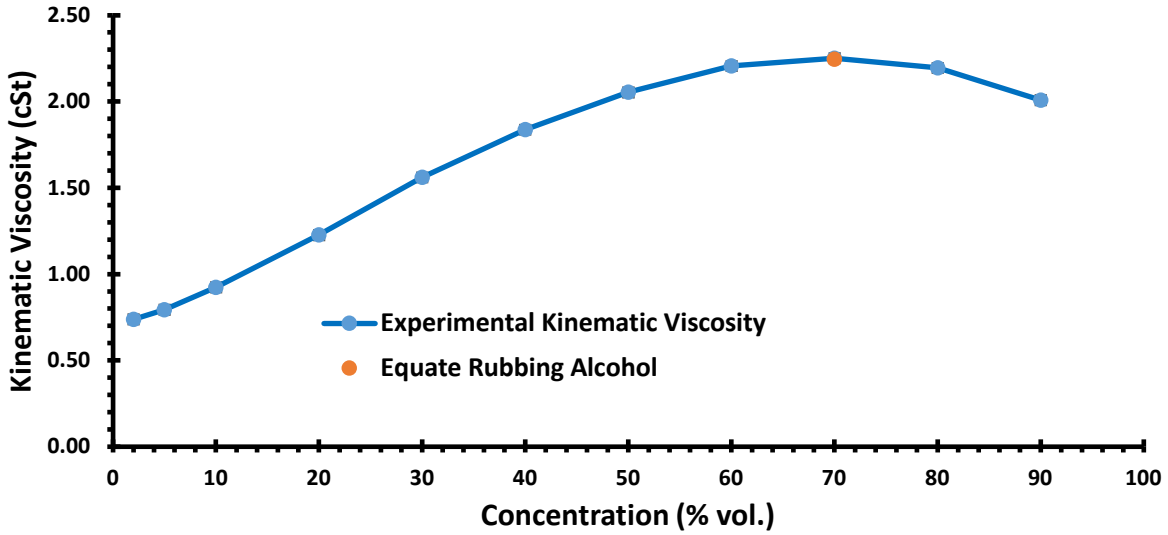

Figure 2-11: Kinematic viscosities of 2-propanol-water mixture as a function of 2-propanol concentration. Kinematic viscosity of a commercial product also plotted.

Kinematic Viscosity of Acetone

The kinematic viscosity of acetone at varying concentrations can be seen in Figure 2-12. This figure shows an increase in kinematic viscosities with increasing acetone concentrations. It should be noted that no commercial product was found containing acetone-water mixture except 100% acetone. Therefore, no test was performed on acetone containing commercial products as per the WG recommendation.

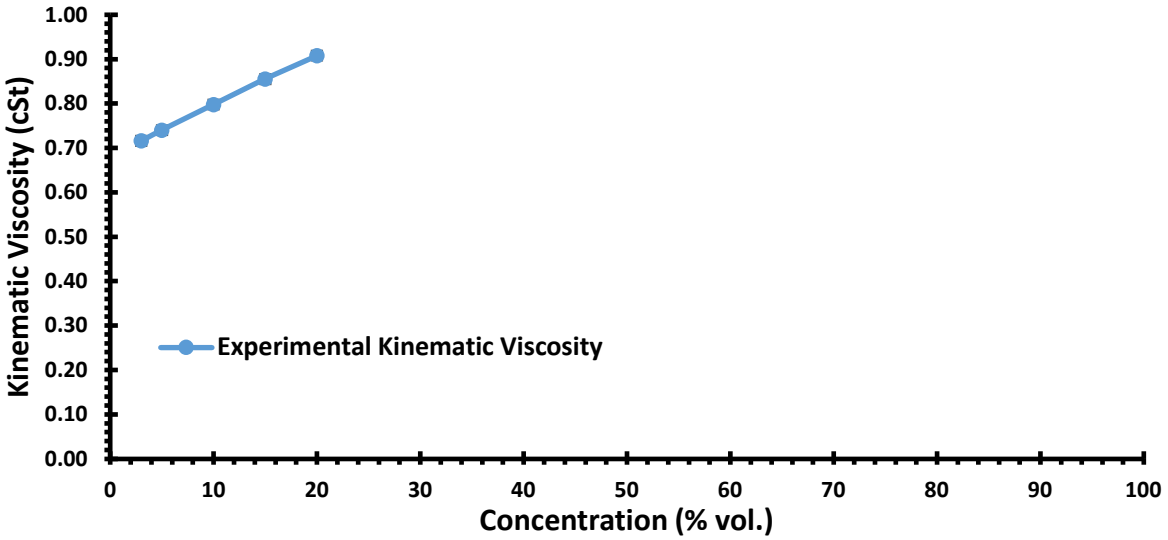

Figure 2-12: Kinematic viscosity of acetone-water mixture as a function of acetone concentration.

Kinematic Viscosity of Acetic Acid

The kinematic viscosity of acetic acid at varying concentrations can be seen in Figure 2-13. This figure shows an initial subtle increase in kinematic viscosities with increasing acetic acid concentrations up to

80%. Later above 80%, this figure shows a decrease in kinematic viscosities with increasing acetic acid concentrations up to 95%. The measured kinematic viscosity of Allen's Double Strength Cleaning Vinegar corresponds to a 10% acetic acid concentration of the acetic acid. It should be noted that the WG did not recommend any test for 10% acetic acid concentration. Hence, no experimental kinematic viscosity of 10% Acetic acid concentration was available to compare with Allen's Double Strength Cleaning Vinegar.

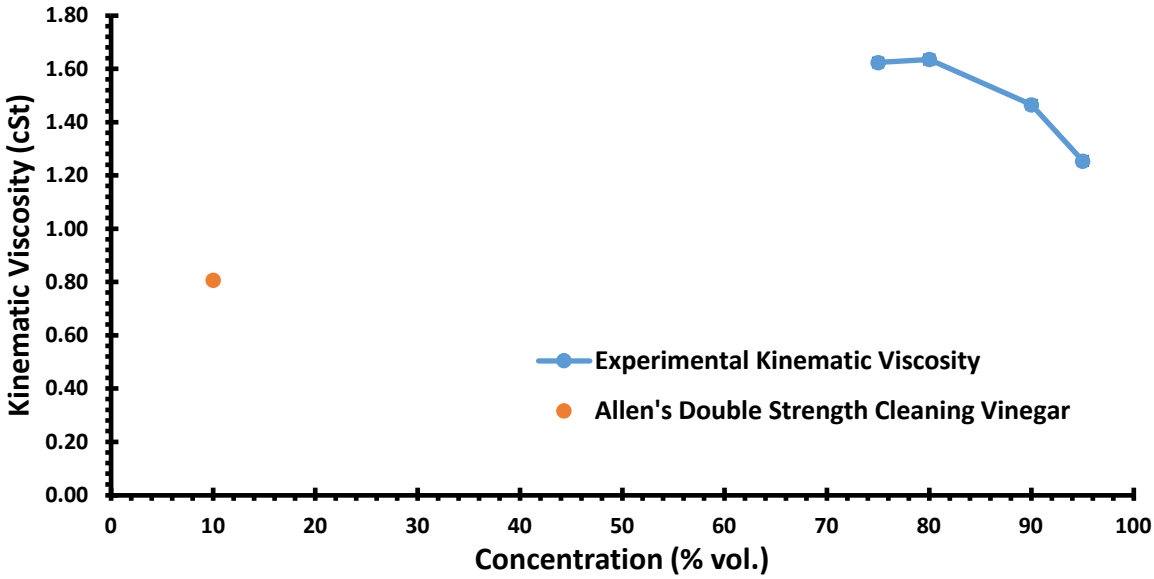

Figure 2-13: Kinematic viscosities of acetic acid-water mixture as a function of acetic acid concentration. Kinematic viscosity of a commercial product also plotted.

2.3.3 Flash and Fire Points

The flash and fire points of methanol, ethanol, 2-propanol, acetone and acetic acid are displayed in the following section. The theoretical flash and fire points are closed cup values obtained from literature, which are compared to the open cup values, i.e. the experimental flash and fire points.

Flash Point of Methanol

The flash point of methanol at various concentrations can be seen in Figure 2-14. This figure shows a decrease in flash points with increasing Methanol concentrations. The measured flash point of the Reflex Windshield Washer Fluid, -49 °C, corresponds to 50% methanol concentration, whereas the Certified Windshield Washer Fluid, -35 °C corresponds to 40% methanol concentration. It should be noted that the Reflex Windshield Washer Fluid up-to-date SDS reported closed-cup flash point was 26.6 °C [4], and the Certified Windshield Washer Fluid up-to-date SDS reported closed-cup flash point was 24–29 °C [5].

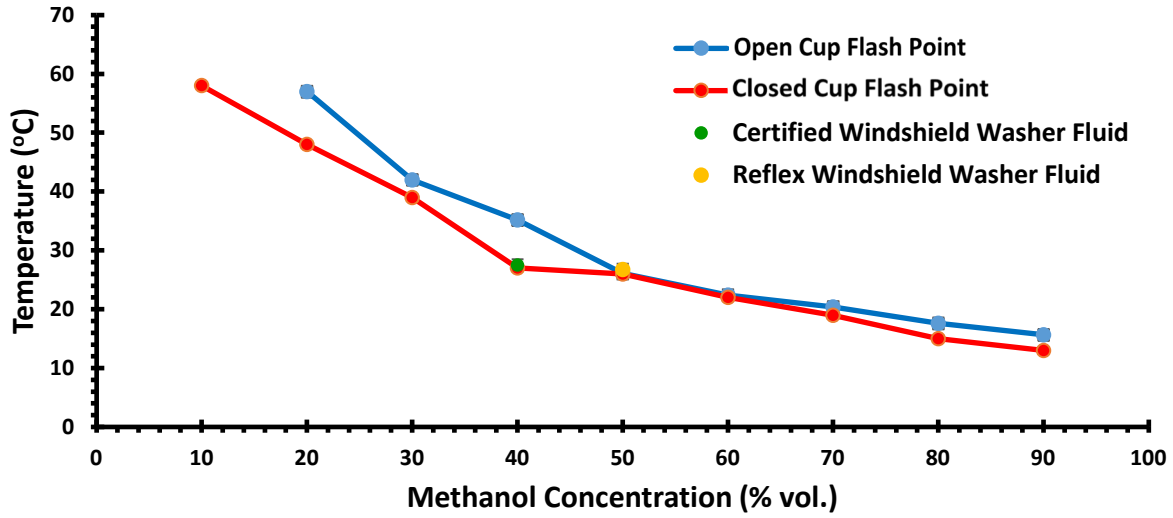

Figure 2-14: Experimental open-cup flash points of methanol-water mixtures with theoretical closed-cup values plotted as a function of methanol concentration [1]. Flash point of two commercial products also plotted.

Fire Point of Methanol

The flash point of methanol at various concentrations can be seen in Figure 2-15. This figure shows a decrease in fire points with increasing methanol concentrations. The measured fire point of the Reflex Windshield Washer Fluid, -49 °C corresponds to 50% methanol concentration, whereas the measured fire point of the Certified Windshield Washer Fluid, -35 °C corresponds to 40% methanol concentration.

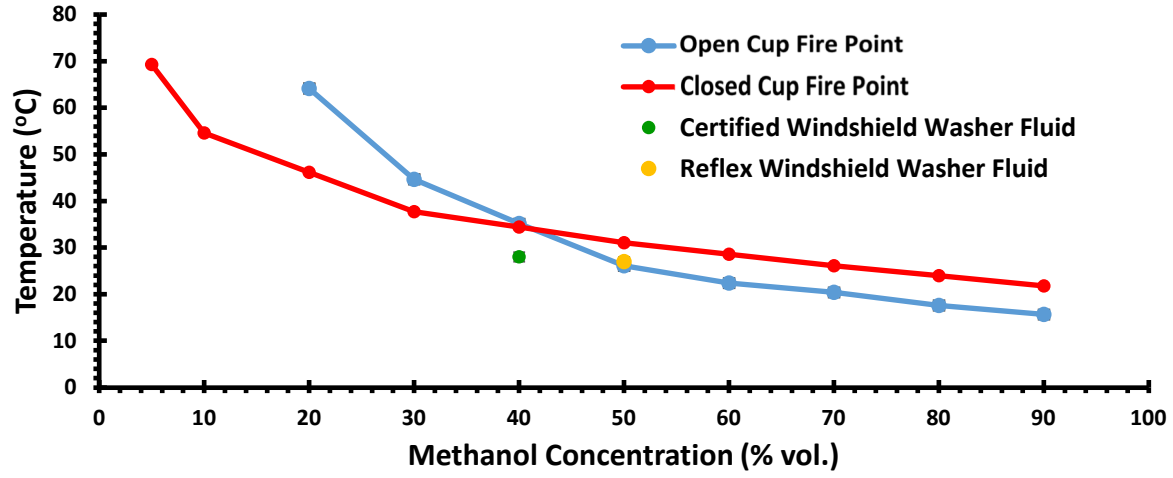

Figure 2-15: Experimental open-cup fire points of methanol-water mixture with theoretical closed-cup values plotted as a function of methanol concentration [1]. Fire point of two commercial products also plotted.

For 40–90% methanol concentrations, the flash and fire point were indistinguishable. This could be rationalized by the high methanol vapour concentrations produced during the experiment for these

methanol concentrations. Therefore, the observed flash points were considered equal to the fire points. For 20–30% methanol concentrations, both flash and fire points were observed. No flash and fire points were observed for 5–10% Methanol concentrations. This could be rationalized by the low methanol vapour concentrations produced during the experiment for these methanol concentrations.

Flash Point of Ethanol

Figure 2-16 shows the flash point of ethanol at various concentrations. This figure shows a decrease in flash points with increasing ethanol concentrations. The measured flash point of the Certified Plumbing Antifreeze, -50 °C, corresponds to 40% ethanol concentration. It should be noted that the Certified Plumbing Antifreeze up-to-date SDS reported closed-cup flash point was 35 °C [6].

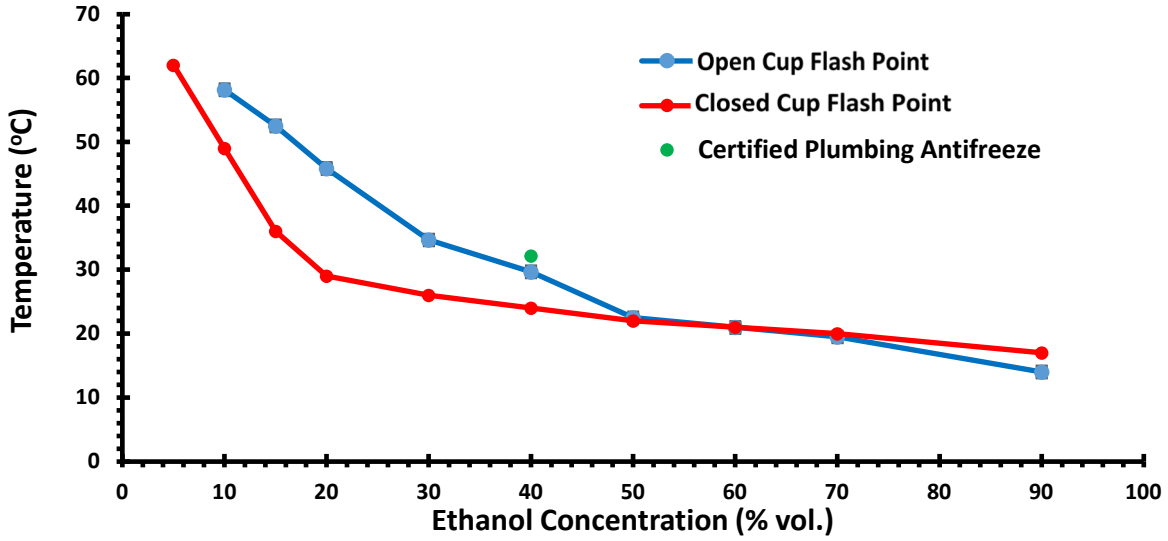

Figure 2-16: Experimental open-cup flash points of ethanol-water mixture with theoretical closed-cup values plotted as a function of ethanol concentration [1]. Flash point of commercial product also plotted.

Fire Point of Ethanol

Figure 2-17 shows the flash point of ethanol at various concentrations. It can be seen that a decrease in fire points with increasing ethanol concentration. The measured fire point of the Certified Plumbing Antifreeze, -50 °C, corresponds to 40% ethanol concentration.

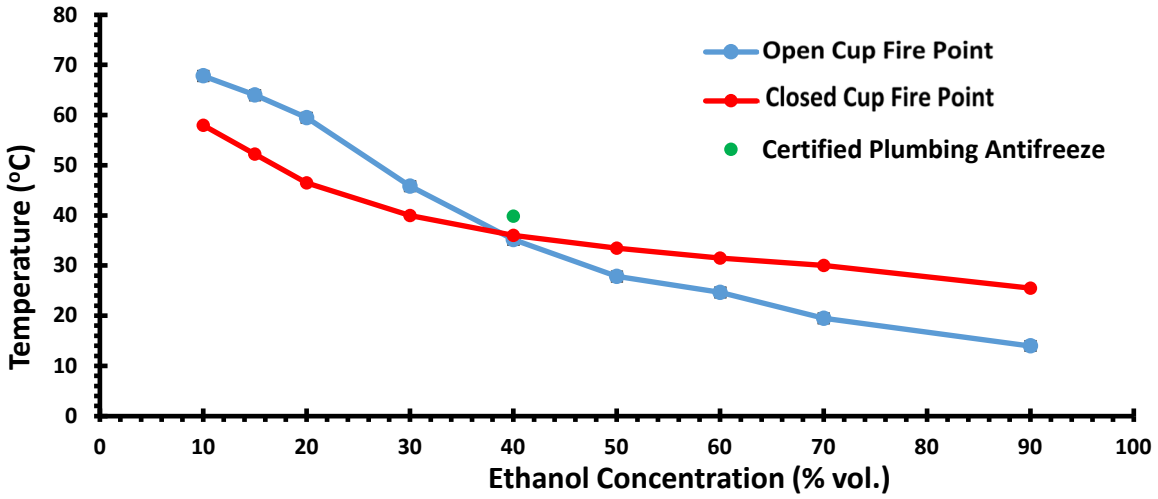

Figure 2-17: Experimental open-cup fire points of Ethanol-Water mixture with theoretical closed-cup values plotted as a function of ethanoll concentration [1]. Fire point of a commercial product also plotted.

Flash Point of 2-Propanol

Figure 2-18 shows the flash point of 2-propanol at various concentrations. A decrease in flash points with increasing 2-Propanol concentrations is seen. The measured flash point of the Equate Rubbing Alcohol corresponds to 70% 2-propanol concentration.

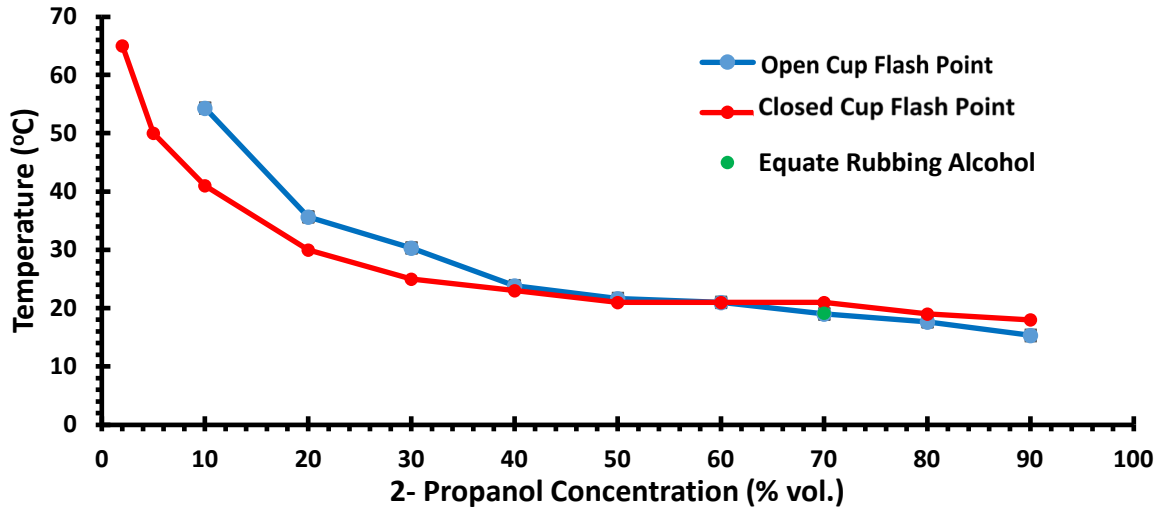

Figure 2-18: Experimental open-cup flash points of 2-propanol-water mixture with theoretical closed-cup values plotted as a function of 2-propanol concentration [1]. Flash point of a commercial product also plotted.

Fire Point of 2-Propanol

Figure 2-19 shows the fire point of 2-propanol at various concentrations. In this figure, a decrease in fire points with increasing 2-Propanol concentrations can be seen. The measured fire point of the Equate Rubbing Alcohol corresponds to 70% 2-propanol concentration.

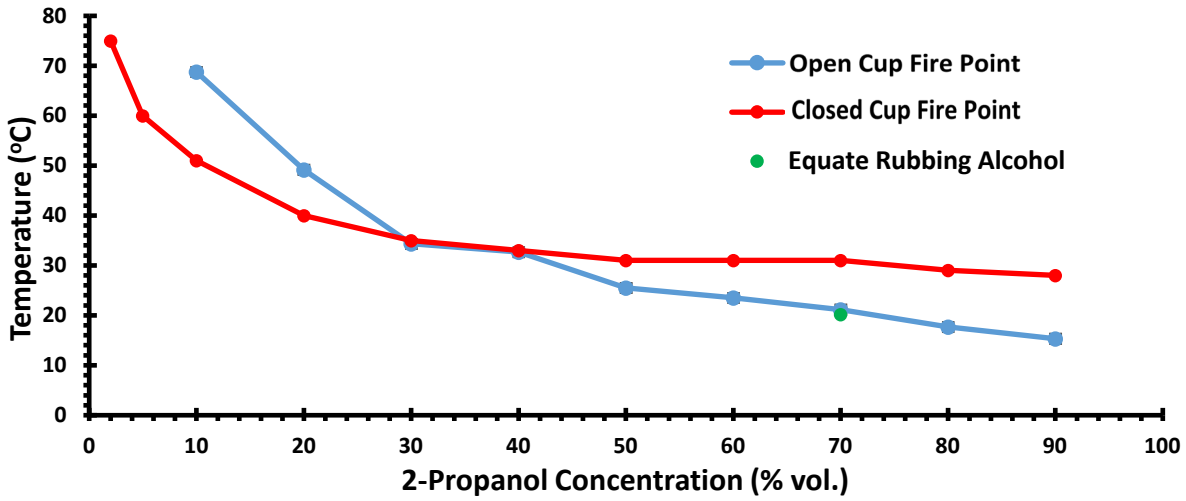

Figure 2-19: Experimental open-cup fire points of 2-propanol-water mixture with theoretical closed-cup values plotted as a function of 2-propanol concentration [1]. Fire point of a commercial product also plotted.

Flash Point of Acetone

Figure 2-20 shows the flash point of acetone at various concentrations. This figure displays a decrease in flash points with increasing acetone concentrations. It should be noted that no commercial product was found containing acetone-water mixture except 100% Acetone. Therefore, no test was performed on acetone containing commercial products as per the WG recommendation.

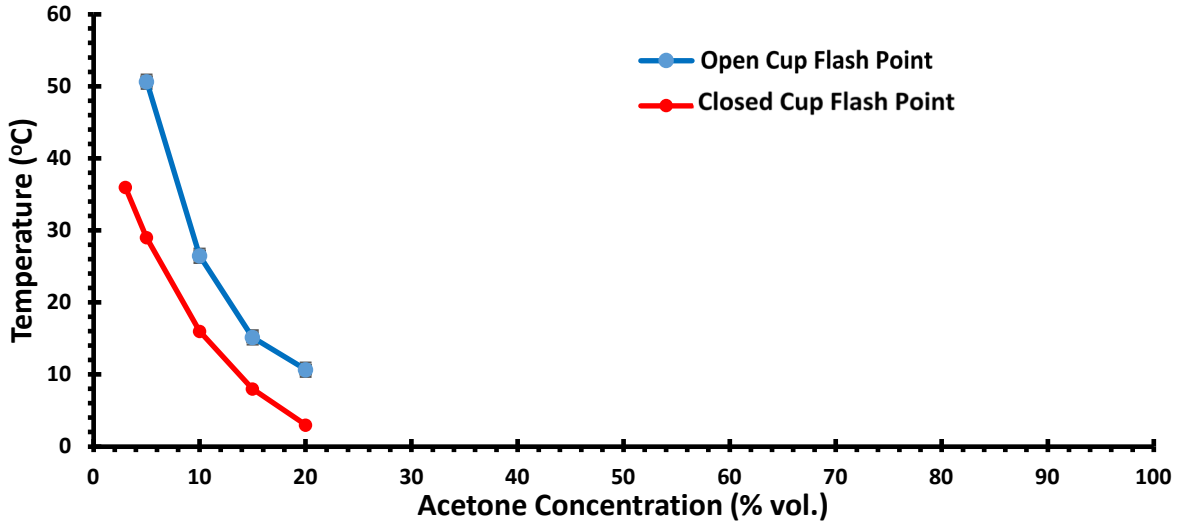

Figure 2-20: Experimental open-cup flash points of acetone-water mixture with theoretical closed-cup values plotted as a function of acetone concentration [1].

Fire Point of Acetone

Figure 2-21 shows the fire point of acetone at various concentrations. In this figure, a decrease in fire points with increasing acetone concentrations. It should be noted that no commercial product was found containing acetone-water mixture except 100% acetone. Therefore, no test was performed on acetone containing commercial products as per the WG recommendation.

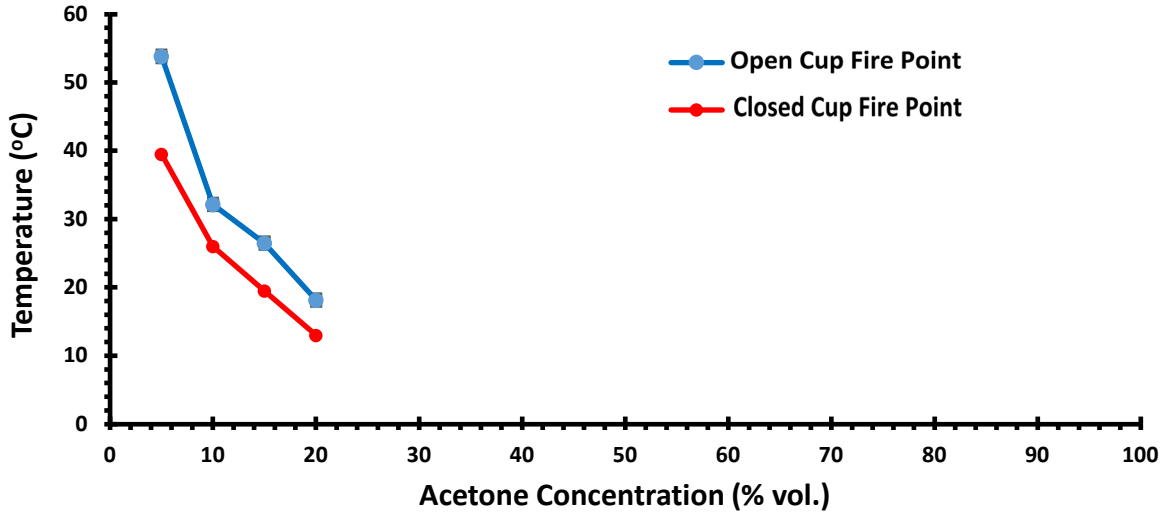

Figure 2-21: Experimental open-cup fire point of acetone-water mixtures with theoretical closed-cup values plotted as a function of acetone concentration [1].

Flash Point of Acetic Acid

Figure 2-22 shows the flash point of acetic acid at various concentrations. In this figure, a decrease in flash points with increasing acetic acid concentrations is displayed. The flash point of Allen's double-strength cleaning vinegar was not found due to it's low concentration of acetic acid (10%).

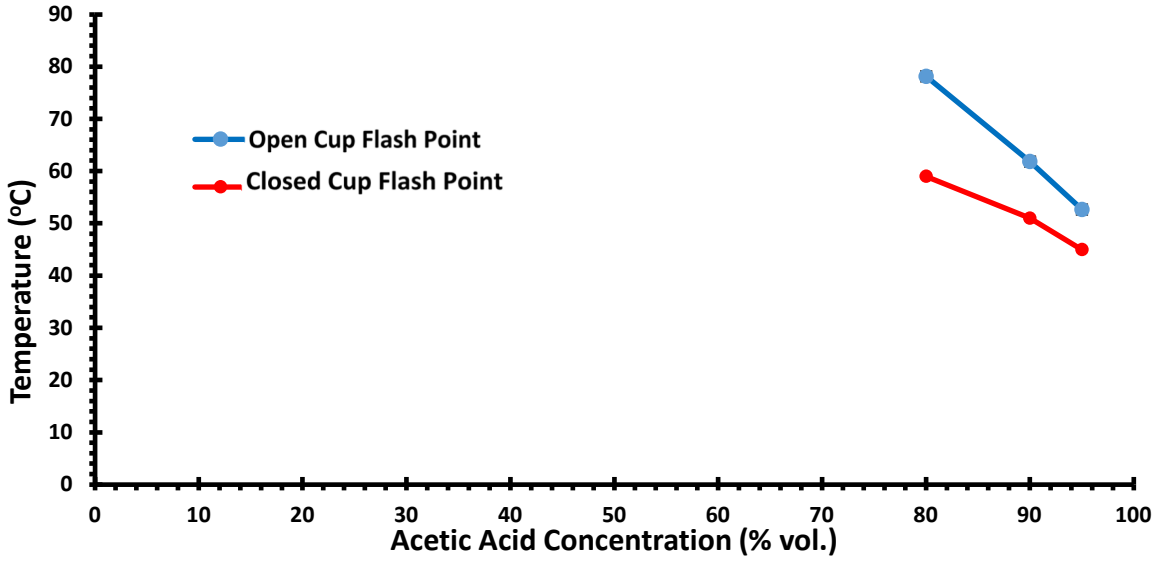

Figure 2-22: Experimental open-cup flash points of acetic acid-water mixture with theoretical closed-cup values plotted as a function of acetic acid concentration [1].

Fire Point of Acetic Acid

Figure 2-23 shows the fire point of acetic acid at various concentrations. In this figure, a decrease in theoretical fire points with increasing acetic acid concentration can be seen. There was no fire point found below a concentration of 95% acetic acid. The fire point of Allen's double-strength cleaning vinegar was not found due to it's low concentration of acetic acid (10%).

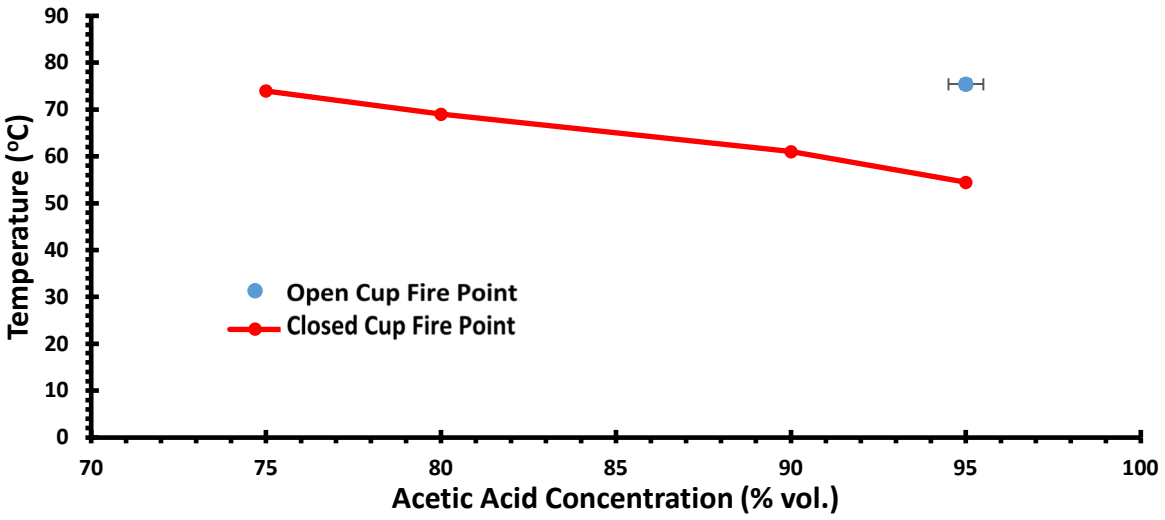

Figure 2-23: Experimental open-cup fire points of acetic acid-water mixtures with theoretical closed-cup values as a function of acetic acid concentration [1].

2.4 Discussion

2.4.1 Boiling Points

The boiling points obtained can be compared with vapour liquid equilibrium data (VLE) found in the literature. By comparing the experimental boiling points to the VLE above data, it was concluded that the boiling point instrument measures the bubble point of the mixture accurately. The bubble point is the temperature at which a single bubble of vapour is formed by the mixture [9]. This value is always lower than the dew point, the temperature at which a single drop of liquid is formed from a completely vaporized system [9].

Figure 2-24 shows that the experimental boiling points of Methanol-Water are similar to the bubble point temperatures found by Kurihara *et al.* [10]. It can also be seen that the boiling point of the Certified Windshield Washer Fluid, -35 °C, containing 40% Methanol was within 0.55 °C of the Methanol-Water mixture and Reflex Windshield Washer Fluid, -49 °C, containing 50% Methanol was within 1.5 °C of the Methanol-Water mixture.

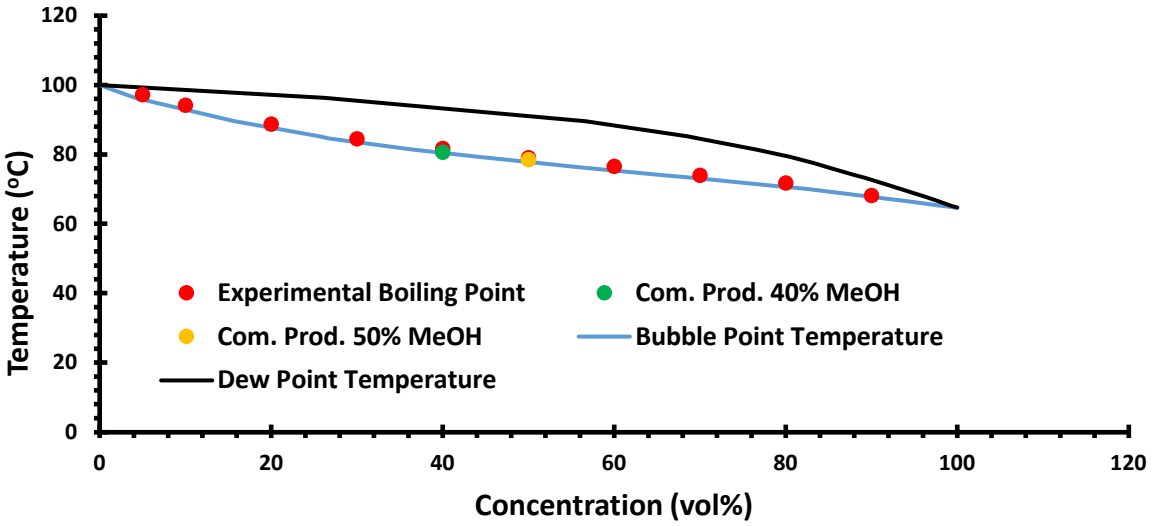

Figure 2-24: Comparison of the experimental boiling point of Methanol-Water and commercial products to VLE data found in the literature.

Figure 2-25 shows that the experimental boiling points of Ethanol-Water are similar to the bubble point temperatures found by Kurihara *et al.* [10]. It can also be seen that the boiling point of the Certified Plumbing Antifreeze, -50 °C, containing 40% ethanol, was within 1.75°C of the Ethanol- Water mixture.

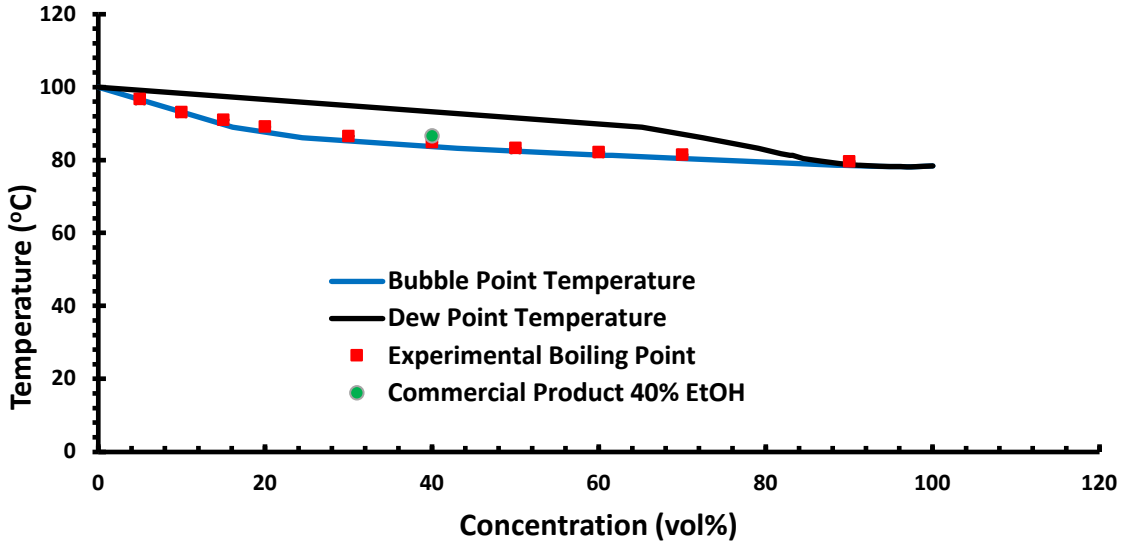

Figure 2-25: Comparison of the experimental boiling point of Ethanol-Water and commercial products to VLE data found in the literature.

Figure 2-26 shows that the experimental boiling points of 2-Propanol-Water are similar to the bubble point temperatures found in Li et al. [11]. It can also be seen that the boiling point of the Equate Rubbing Alcohol containing 70% 2-Propanol was within 0.5°C of the 2-Propanol-Water mixture.

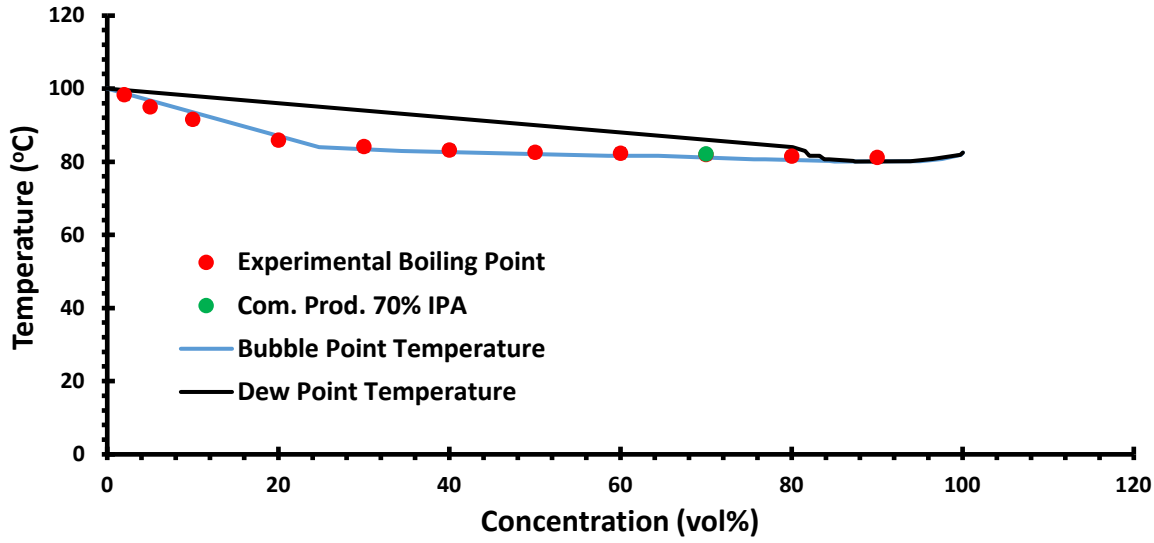

Figure 2-26: Comparison of the experimental boiling point of 2-propanol-water and commercial product to VLE data found in the literature.

Figure 2-27 shows that the experimental boiling points of acetone-water are similar to the bubble point temperatures found by Al-Sahhaf *et al*. [12].

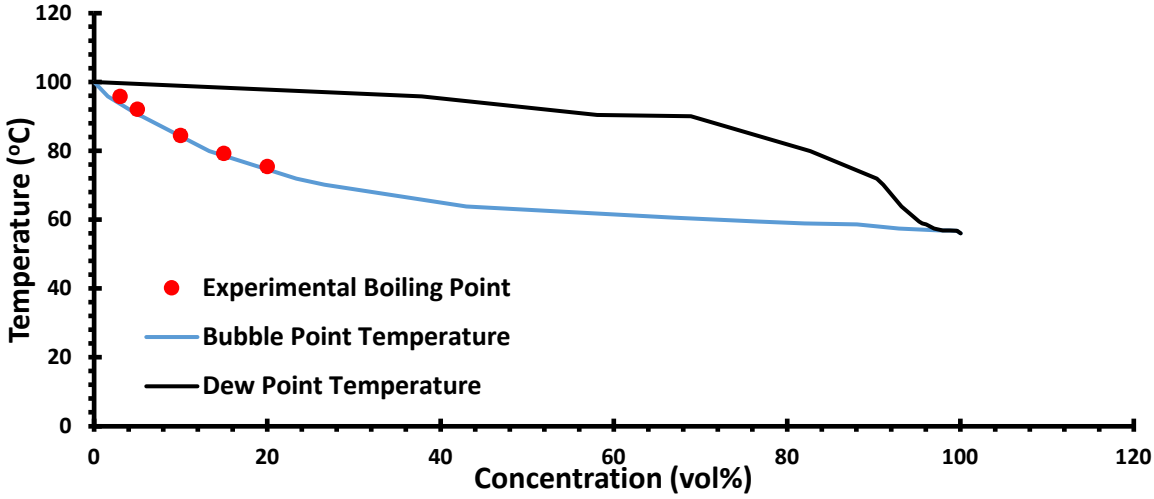

Figure 2-27: Comparison of the experimental boiling point of acetone-water to VLE data found in the literature.

Figure 2-28 shows that the experimental boiling points of acetic Acid-water are similar to the bubble point temperatures found by Zhang et al. [13]. Allen's Double Strength Cleaning Vinegar cannot be compared since a 10% acetic acid-water mixture was not produced.

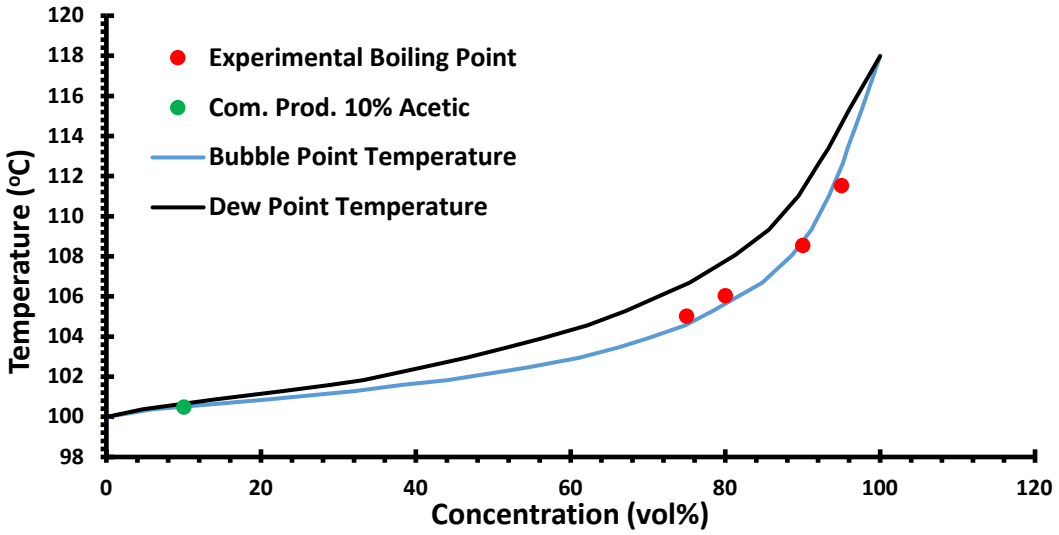

Figure 2-28: Comparison of the experimental boiling point of acetic acid-water and commercial product to VLE data found in the literature.

2.4.2 Kinematic Viscosities

Theoretical kinematic viscosities were obtained from several literature sources [14-17,18,19]. All of the kinematic viscosities were obtained at a temperature of 40°C, except for acetone-water, which was obtained at 37.8°C. Due to the fact that all the literature sources reported kinematic viscosities at the mole fraction (or mole percent) of the mixture, they were converted into volume percent to allow for comparison. In Figure 2-29, the 2-propanol-water mixture is shown to reach a maximum at about 64.5 % volume, while in Figure 2-30, the maximum occurs at about 70 % volume. The ethanol-water mixture is shown to reach a maximum between 50 and 60 % volume in Figure 2-29, while the maximum occurs at about 60 % volume in Figure 30. The Acetic Acid-Water mixture is shown to decrease from 75 % volume to 96 % volume in Figure 2-29, while in Figure 2-30, the mixture increases slightly from 75 to 80 % volume, followed by a decrease to 95 % volume. In Figure 2-29, the methanol-water mixture reaches a maximum at about 69 % volume, while in Figure 2-30, the maximum is reached at about 50 % volume. Lastly, the mixture of acetone-water is shown to increase from 3 up to about 20 % volume in Figure 2-30, which can also be seen in Figure 2-29.

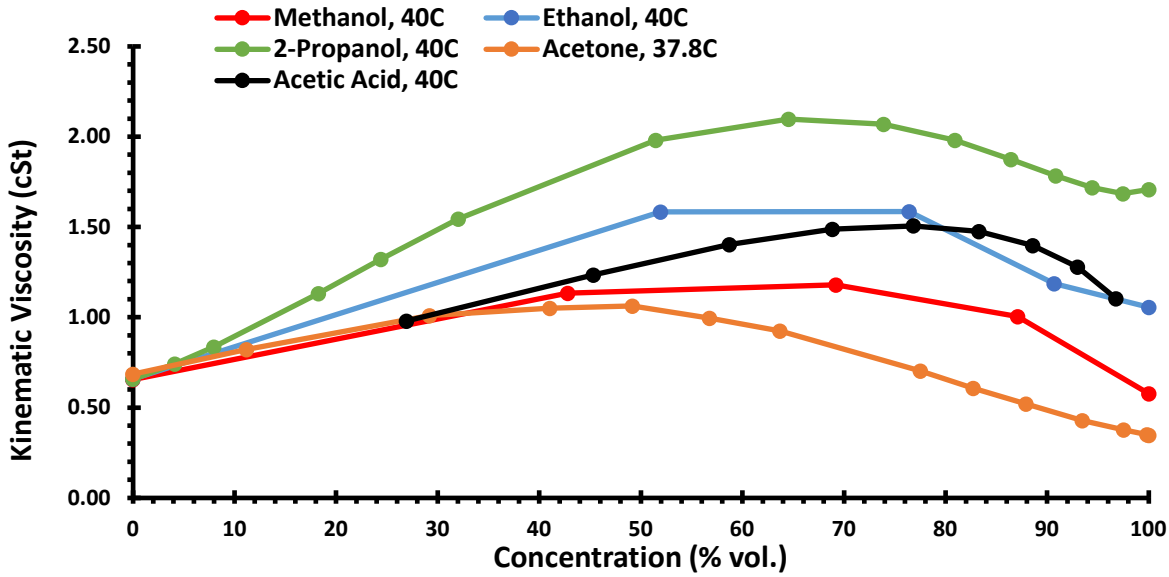

Figure 2-29: Combined plot of kinematic viscosities obtained from the literature.

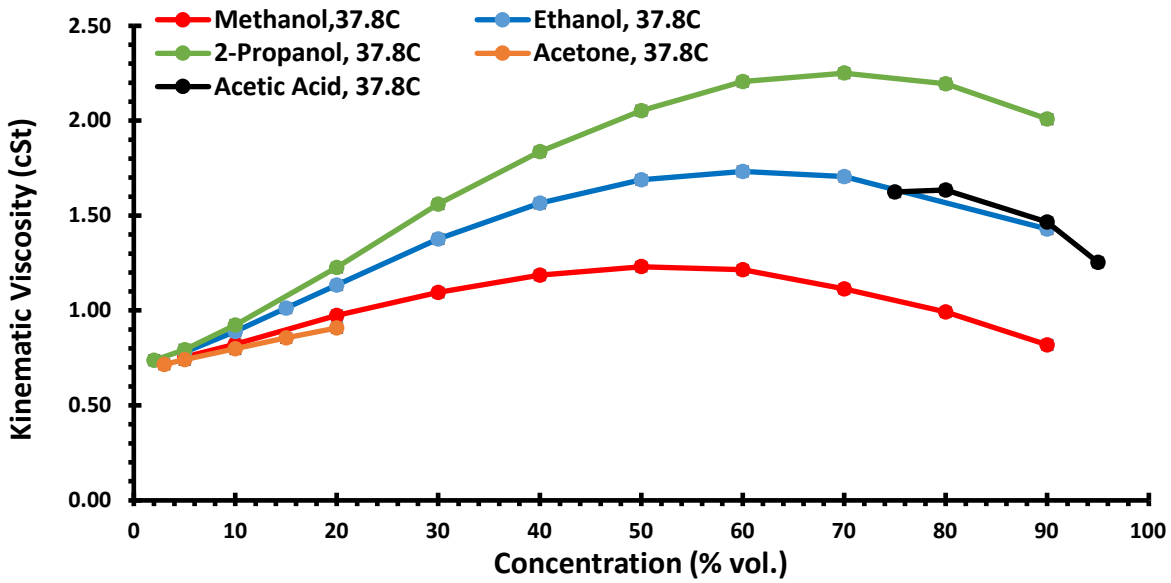

Figure 2-30: Combined plot of experimental kinematic viscosities.

The kinematic viscosities of the Certified Windshield Washer Fluid, -35 °C, which contains 40 % volume methanol and Reflex Windshield Washer Fluid, -49 °C, which contains 50 % volume methanol was shown to be very close to their respective methanol-water mixtures – both were within 0.1 cSt. The kinematic viscosity of the Certified Plumbing Antifreeze, -50 °C, which contains 40 % volume ethanol was also very close to the ethanol-water mixture – the difference is within 0.05 cSt. The Equate Rubbing Alcohol, which contains 70 % volume 2-propanol, was almost an exact match to the 2-propanol-water mixture, with a difference of only 0.005 cSt. A comparison cannot be made for Allen's Double Strength Cleaning Vinegar since a synthetic mixture of 10 % volume acetic acid was not tested.

2.4.3 Flash and Fire Points

The flash and fire point of a liquid occurs when enough vapour is formed above the liquid to produce a flammable environment [20]. The partial pressure of flammable vapours above the liquid must be equal to the lower flammability limit (LFL) of the liquid. If only a single component of the mixture is flammable, such as the WMFL-Water mixtures in this report, the non-flammable species will be present in the vapour phase, which reduces the local partial pressure and increases the flash/fire point [20]. When there is water present at a high concentration, not only is the partial pressure of flammable vapour reduced, but the local partial pressure of oxygen is also reduced. Therefore, even if the vapour is above the LFL, there might not be enough oxygen to burn, and a flash/fire point will not be found [12]. For example, in the case of methanol, the flash/fire point was not observed at 10 % volume or 5 % volume. The flash/fire point of ethanol was observed at 10 % volume but not at 5 % volume. Similar observations were found with 2-Propanol and Acetone.

At low concentrations, the open cup flash and fire points should be greater than the theoretical closed cup values obtained from the literature. During open-cup testing, the flammable vapours are constantly diffusing into the open atmosphere. As a result, the local partial pressure of the flammable vapour is always lower than the partial equilibrium pressure that would be present in a closed environment. As the

concentration of WMFL increases, the amount of vapour being produced should reach a point where the diffusion of the flammable vapours has a much lower effect. As a result, the local partial pressure would be closer to the equilibrium value seen in a closed cup experiment, and a flash and fire point resembling the closed cup flash and fire point would be found. This is seen in Figures 2-14,2-16, and 2-18, where the flash points are greater than the theoretical values at low concentrations, but as the concentration increases, they become closer in value. In Figures 2-15, 2-17 and 2-19, the fire points are higher than the theoretical values at lower concentrations, which is expected. However, at high concentrations, the fire point is significantly lower than the theoretical value, which is unexpected and may be due to the sources of error that will be discussed further. In Figures 2-20, 2-21 and 2-22, the flash and fire points are all higher than the theoretical values, which, as stated earlier, is expected. Figure 2-23 shows only a single fire point (Acetic Acid- Water, 95 % vol.), which is much greater than the theoretical value – a gap of this magnitude may be due to the sources of error that will be discussed.

The flash and fire point of the Equate Rubbing Alcohol was within 1^{o}C of the 2-propanol-water mixture (70 % vol.). The Reflex Windshield Washer Fluid, -49 ^{o}C, flash and fire point were within 1^{o}C of the methanol-water mixture (50 % vol.). The Certified Windshield Washer Fluid, -35 ^{o}C flash-point was lower than the methanol-water mixture (40 % vol.) by around 7.7 ^{o}C, and the fire point was 7.2 ^{o}C lower. For the Certified Plumbing Antifreeze, -50 ^{o}C, the flash-point was 2.4^{o}C lower, and the fire point was 6^{o}C lower than the ethanol-water mixture (40 % vol.).

2.4.4 Sources of Error

Random errors affect precision, which is how reproducible measurement is under the same circumstances. Systematic error affects the accuracy of measurement or how close the observed value is to the true value. For boiling point and viscosity determination, there are almost no random or systematic errors associated with the instruments. The viscometer and boiling point tester are automated instruments; therefore, if the instruments are programmed correctly (heating rates, temperature, etc.), the values obtained are precise and accurate. However, there could be errors associated with sample preparation. The open-cup flash point tester is where both the random and systematic error lies since this device relies heavily on human interaction and visual determination of the flash/fire point. For example, the size of the pilot flame significantly impacts the flash/fire point, which may vary slightly from experiment to experiment and is, therefore, a random error. A flame that is too large will result in an underestimation of the flash/fire point, i.e., the vapor will ignite easier. A flame that is too small will overestimate the flash/fire point because it will be more difficult to produce ignition. The liquid level also plays a role in the flash/fire point measurements. It was found that even a deviation of a few millimetres could impact the results. This random error is more noticeable at higher concentrations where the flash and fire points deviate from the expected results quite substantially. This is because at lower concentrations, since the amount of vapor being produced is so low, the distance to the flame plays less of a role. At high concentrations, there is enough vapor being released for the distance to make less of a difference. Lastly, since binary mixtures of water and volatile species were used, the concentration of the mixture changes as the experiment is underway due to the more volatile component vaporizing faster than the water. This is a systematic error that results in an overestimation of the flash/fire point. As the volatile component vaporizes and the concentration decreases, less vapor is formed over time, and therefore a higher temperature is required to reach the flash/fire point. Similarly, the liquid level decreases as the experiments are underway due to vaporization, which is a systematic error resulting in an overestimation of the flash/fire point because the distance from the flame increases.

2.5 Conclusion

This chapter discusses the determination and analysis of boiling point, kinematic viscosity, flash point and fire point of five WMFL-Water mixtures at various concentrations and five commercial products that contain some of these WMFLs. This information will be used to update the National Fire Code to lower the burden currently placed on the construction industry. Boiling points and kinematic viscosities follow the expected trends found in the literature, and minimal errors are associated with these tests. Open cup flash and fire points followed the expected trends in some cases, with deviations being found at higher concentrations. These deviations may be due to the sources of error which were previously discussed.

2.6 Recommendations

Using an automated, closed-cup instrument for binary mixtures is recommended due to the previously stated errors or a modified version of the ASTM standard to reduce the composition and liquid level variation as the experiment progresses. This modified methodology would initially obtain an estimate of the flash/fire point using the current ASTM standard and then complete an additional three trials by redoing the experiment, this time 2-3 ^{o}C below the estimate that was found. Since the experiment would be started only a few degrees below the expected flash/fire point, there would be less time for the concentration/level to decrease.

References

[1] R. Hassan, "Determination of physical properties of water-miscible flammable liquid mixtures - Phase 1", National Research Council Canada, 2019.

[2] P. J. Martínez, E. Rus and J. M. Compaña, “Flash point determination of binary mixtures of alcohols, ketones and water”, University of Malaga, 2005.

[3] National Research Council, "National fire code of Canada", http://Www.Nrc-Cnrc.Gc.Ca/Eng/Ibp/Irc/Codes/05-National-Fire-Code.Html, 2010.

[4] Recochem Inc., Montreal, Canada, "Reflex Windshield Washer Fluid, -49 °C: Safety Data Sheet", 2017.

[5] Recochem Inc., Montreal, Canada, "Certified Windshield Washer Fluid, -35 °C: Safety Data Sheet", 2017.

[6] Recochem Inc., Montreal, Canada, "Certified Plumbing Antifreeze, -50 °C: Safety Data Sheet", 2017.

[7] Equate 70% Isopropyl Alcohol, https://www.walmart.com/ip/Equate-70-Isopropyl-Alcohol-32-Oz/192925013.

[8] Allen's Double Strength Cleaning Vinegar, https://www.walmart.ca/en/ip/allens-double-strength-cleaning-vinegar/6000196262681.

[9] M. Abbot and H. Ness, "Introduction to Chemical Engineering Thermodynamics", McGraw-Hill Education, 2019.

[10] K. Kurihara, M. Nakamichi, K. Kojima, "Isobaric Vapor-Liquid Equilibria for Methanol + Ethanol + Water and the Three Constituent Binary Systems", J. Chem. Eng. Data. 38, pp.446–449, 1993. https://doi.org/10.1021/je00011a031.

[11] Q. Li, F. Xing, Z. Lei, B. Wang, Q. Chang, "Isobaric vapor-liquid equilibrium for isopropanol + water + 1-ethyl-3-methylimidazolium tetrafluoroborate", J. Chem. Eng. Data. 53, pp. 275–279, 2008. https://doi.org/10.1021/je7003808.

[12] T.A. Al-Sahhaf, N.J. Jabbar, "Vapor-Liquid Equilibrium of the Acetone-Water-Salt System", pp. 522–526, 1993.

[13] Zhang, H. Wan, L. Xue, G. Guan, "Investigation on isobaric vapor liquid equilibrium for acetic acid+water+(n-propyl acetate or iso-butyl acetate)", Fluid Phase Equilib. 305, pp. 68–75, 2011, https://doi.org/10.1016/j.fluid.2011.03.006.

[14] M. S. Alam, B. Ashokkumar, A. M. Siddiq, "The density, dynamic viscosity and kinematic viscosity of protic polar solvents (pure and mixed systems) studies: A theoretical insight of thermophysical properties," *Journal of Molecular Liquids*, vol. 251, pp. 458–469, 2018.

[15] Y. Qiao, Z. Di, Y. Ma, P. Ma, S. Xia, Viscosities of pure water, acetic acid + water, and p-xylene + acetic acid + water at different temperature and pressure, Chinese J. Chem. Eng. 18 (2010) 446–454. https://doi.org/10.1016/S1004-9541(10)60242-X.

[16] J.G. Bleazard, T.F. Sun, A.S. Teja, The thermal conductivity and viscosity of acetic acid-water mixtures, Int. J. Thermophys. 17 (1996) 111–125. https://doi.org/10.1007/BF01448214.

[17] K. Noda, M. Ohashl, "Viscosities and densities at 298.15 K for mixtures of methanol, acetone, and water", Shizuoka University, 1982.

[18] K.S. Howard, R.A. McAllister, "The viscosity of acetone-water solutions up to their normal boiling points", AIChE , pp.362–366, 1958, https://doi.org/10.1002/aic.690040326.

[19] F.M. Pang, C.E. Seng, T.T. Teng, M.H. Ibrahim, "Densities and viscosities of aqueous solutions of 1-propanol and 2-propanol at temperatures from 293.15 K to 333.15 K", J. Mol. Liq. 136, pp. 71–78, 2007, https://doi.org/10.1016/j.molliq.2007.01.003.

[20] G.R. Astbury, E. Grollet, K.M. Stell, "Flash points of aqueous solutions of flammable solvents", Ecole des Mines d'Albi, 2004.

[21] Janès and J. Chaineaux, "Experimental determination of flash points of flammable liquid aqueous solutions", *The Italian Association of Chemical Engineering*, 2013.

Fox M.A, "Flammable liquids and class 3", Glossary for the Worldwide Transportation of Dangerous Goods and Hazardous Materials, 1999. https://doi.org/10.1007/978-3-662-11890-0_33

Chapter 3. A Novel Method of Membrane Characterization Using Steady State Step Changes

Abstract

Gas separation membranes have been used as an alternative to absorption, cryogenic distillation, adsorption and other complex unit operations. The reason for this is their simplicity, cost-effectiveness and efficiencies offered. Polymeric membranes dominate the industry because they have good selectivity and permeability, are easy to synthesize and are mechanically stable.

Membrane characterization, i.e. obtaining the fundamental transport properties of a membrane, is usually done using the time lag method in a constant volume (CV) system. The time-lag method allows the determination of the permeability, diffusivity and solubility in polymeric gas separation membranes from a single dynamic gas permeation experiment. The time lag method involves exposing a membrane that is originally degassed to a sudden increase in pressure upstream. The rate of pressure increase in the downstream receiving volume is monitored, which produces a pressure rise curve which can be used to extract the membrane properties. For the complete characterization of glassy polymer membranes, which are commonly used in the industry, multiple time lag experiments are required at varying pressures. This is because, in addition to the permeability, diffusivity and solubility coefficients, glassy polymeric membranes require the determination of other parameters such as the affinity coefficient, Langmuir sites capacity, diffusivity in the Langmuir sites and the equilibrium constant between the Langmuir and Henry's sites.

A novel time-lag protocol is proposed based on a series of step changes in the feed pressure (steps up followed by steps down), equivalent to multiple time lag experiments. Unlike the classical time-lag protocol, the initial condition for the characterized membrane in the new protocol is a linear concentration profile within the membranes instead of a uniform zero concentration across the membrane.

This novel protocol was tested using laboratory-made dense polyphenylene oxide (PPO) membranes. Time lags at different steps were within 5-20% of each other, which was expected for a glassy polymer such as PPO. The difference between the first time lag (from the first pressure step) was more significant comparing the subsequent steps. It was most likely due to the difference in initial conditions, i.e. a zero concentration gradient in the membrane for the first step, followed by a linear concentration gradient in the membrane for the subsequent steps.

Nomenclature

Nomenclature

A: Cross-sectional area of membrane (cm^2)

D: Diffusion coefficient of gas in membrane ($cm^2\ s^{-1}$)

M: Molar mass ($kg\ mol^{-1}$)

p : Pressure (Pa)

P: Permeability coefficient of gas in membrane (Barrer)

p_o: Initial pressure (Pa)

Q: Gas flow rate ($kmol\ s^{-1}$)

R: Gas constant ($J\ K^{-1}mol^{-1}$)

S: Solubility of gas in membrane ($cm^3(STP)/(cm^3 \times cmHg)$)

t: Time (s)

T: Absolute temperature (K)

V: Volume of receiver (cm^3)

C: Concentration of gas in the membrane ($mol\ L^{-1}$)

x: Position in membrane (ranges from x=0 to x=L)

C_1: Concentration of gas at feed side of membrane (mol/cm^3) at x=0

C_1: Concentration of gas at permeate side of membrane (mol/cm^3) at x=L

L: Thickness of membrane (micron)

C_D: Gas concentration in Henry's sites ($mol\ L^{-1}$)

C_H: Gas concentration in Langmuir's sites ($mol\ L^{-1}$)

C'_H: Hole saturation constant

b: Hole affinity constant

Greek Symbols:

θ: Time lag of receiver (s)

3.1 Introduction

Gas separation membranes have gained popularity in industrial processes due to their simplicity and cost-effectiveness. Other gas separation processes, such as cryogenic distillation, adsorption, absorption, etc., can be energy intensive and cause environmental damage concerning the disposal of toxic chemicals/adsorbents. A membrane is a thin semipermeable layer that allows for the separation of one or more components from a mixture by selectively allowing the transport of one chosen component using a specific driving force[1]. The species passing through the membrane are referred to as the permeate, while those unable to pass through are referred to as the retentate[1]. However, no separation process can be perfect/ideal- some impurities will always pass through into the permeate, and some products will be found in the retentate[2]. Most of the work related to gas separation membranes is on synthetic polymers since they can be formulated to endure high mechanical, thermal and chemical strain[3].

Polymeric membranes can be either dense (nonporous) or porous, which depends on their pore size[4]. Porous membranes can be broken down into categories based on their respective transport mechanism. If the pores are relatively large – from 0.1 to 10μm – gases permeate the membrane by convective flow, and no separation occurs[4]. If the pores are smaller than 0.1μm and the pore diameter is smaller than the mean free path of the gas molecules, Knudsen diffusion is the mode of transport[4]. Lastly, if the membrane pores are extremely small, on the order of 5 – 20Å, then gases are separated by molecular sieving[4]. Microporous membranes are a topic of interest; however, nonporous or dense membranes dominate the industry and receive more attention. Gas separation through a dense membrane follows the solution-diffusion mechanism because there are no continuous pores for gases to pass through[4].

Depending on the type of material, a porous or nonporous polymeric membrane can be described as either glassy or rubbery, which depends on whether the membrane at ambient temperature is above (rubbery) or below (glassy) its glass transition temperature[5]. Generally, glassy polymers demonstrate high selectivity and low permeability, whereas rubbery polymers behave in the opposite manner - they show high permeability and low selectivity[5]. The structure of a glassy polymer is more rigid, so its molecular chains act as obstacles for gas molecules to pass through, which results in low permeabilities[5]. On the other hand, rubbery polymers have more flexible chains allowing gas molecules to diffuse through them with less resistance[5]. As a result, the permeability will increase, but selectivity is sacrificed since this higher permeability will hold not just for the most permeable gas but also for all gases in the feed mixture.

Developing new membranes with novel properties depends on the ability to reliably test their properties– hence the importance of membrane characterization experiments. The term membrane characterization refers to experiments used to obtain the transport properties of membranes [3]. Since gas transport in dense, polymeric membranes is governed by the solution-diffusion mechanism, the most important properties of a membrane are permeability (P), diffusivity (D) and solubility (S) coefficients. Permeability is the measure of membrane productivity. Solubility indicates the affinity of the gas species to the membrane material, which is indicated by the condensability of gas molecules on the membrane surface. In contrast, the diffusion coefficient represents the speed of molecules passing through the membrane matrix[3]. These three properties are related through equation 3.1 shown below, known as the solution-diffusion model.

$$P = D \cdot S \qquad 3.1$$

Permeability is often measured in the units of "Barrer," which is defined below in equation 3.2.

$$1\ Barrer = 10^{-10}\frac{cm_{STP}^2 \cdot cm}{cm^2 \cdot s \cdot cmHg} = 3.35 \times 10^{-16}\frac{mol \cdot m}{m^2 \cdot s \cdot Pa} \qquad 3.2$$

Two main experimental setups are used for membrane characterization: the constant volume (CV) system and the constant pressure (CP) system.

3.1.1 Constant Pressure System

In a constant pressure system, the permeate side of the membrane is maintained at a constant pressure, which is usually atmospheric. The pressure can also be maintained by using a sweep gas on the permeate side at a constant pressure. This system design allows steady-state experiments to be conducted where the upstream and downstream pressure can remain constant. One downside of the constant pressure system is the possibility of back diffusion from the permeate side to the feed side of the membrane[6]. This may occur if the sweep gas or stagnant gas on the permeate side is composed of species not present in the feed gas[6]. Another downside of the constant pressure system is the difficulty of performing dynamic gas permeation experiments[7]. As a result, it isn't easy to obtain the membrane properties using this type of system. It is especially true for barrier polymers, which are polymers associated with very low permeabilities[7]. The definition of a low permeation rate, also known as a microflow, is usually accepted to be less than 0.1 cm^3(STP)/min. However, permeation rates greater than 1 cm^3(STP)/min have also been classified as microflows[8]. Because most commercial volumetric or mass flow meters have a lower measurement limit of 0.1 cm^3(STP)/min, constant pressure systems are of little use in this application[7]. A simple diagram of a constant pressure system with a sweep gas is shown below in Figure 2.1 [9].

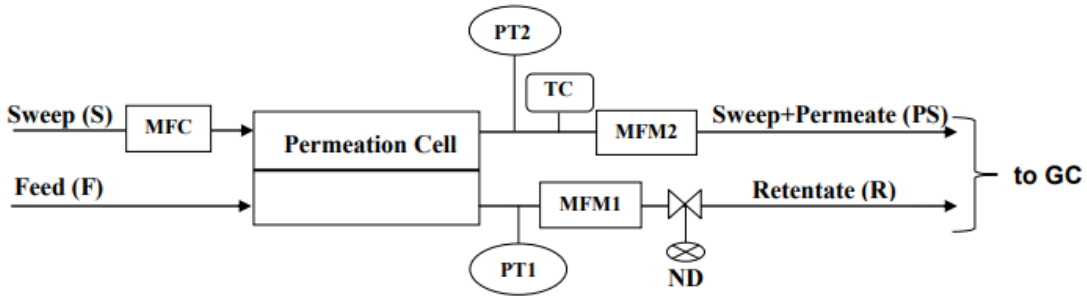

Figure 3-1: Diagram of a constant pressure system with sweep gas, where flow measurements can be taken using the mass flow meters (MFC) and composition can be measured using gas chromatography (GC). "PT" and "TC" refer to pressure and temperature transmitters.

3.1.2 Constant Volume System

In a constant volume (CV) system, the volume of the downstream receiver is known, and the rate of pressure rise is monitored[3]. The permeate side of a CV system is initially at vacuum, allowing for minimal dp/dt measurements to be made accurately. In other words, a CV system overcomes the microflow challenges associated with the CP system discussed above[3]. In addition, CV systems allow for step changes in feed pressure, which is required for performing dynamic gas permeation experiments.

Assuming the applicability of the ideal gas law, the permeation rate (Q) is directly proportional to the rate of pressure increase due to permeating gas in the downstream receiver[3]:

$$Q = \frac{V}{RT}\frac{dp}{dt} \qquad 3.3$$

Equation 3.3 shows the volume (V), ideal gas constant (R), the absolute temperature (T) and the derivative of pressure with respect to time (dp/dt).

The setup consists of a working volume, a reference volume, manual/actuated valves, pressure transmitters, the membrane cell and a vacuum pump.

3.1.3 Determining Membrane Properties with the Time Lag Method

The time lag method involves exposing a membrane that is initially degassed to a sudden increase in pressure upstream. The pressurized gas makes its way to the membrane surface, adsorbs into the membrane, diffuses through the membrane and desorbs into the downstream volume, which is near vacuum conditions. The rate of pressure increase in the downstream receiving volume is monitored, and a pressure response curve is obtained. The figure shown below is a generic pressure rise curve. It can be seen that the pressure response is a transient process and eventually reaches a steady state; typically, this steady state region occurs between 2.5-3 time lags[3]. The time lag is the intersection of the steady state portion of the curve with the x-axis, shown as time t_0 or Θ in the figure below. In reality, the rate of pressure increase is not constant, and it will continue to decrease as the pressure increases in the downstream receiver, which decreases the driving force for gas permeation. Therefore, what is referred to as the steady state is a pseudo-steady-state. However, in a properly designed CV, a decrease in the driving force is negligible compared to its absolute value.

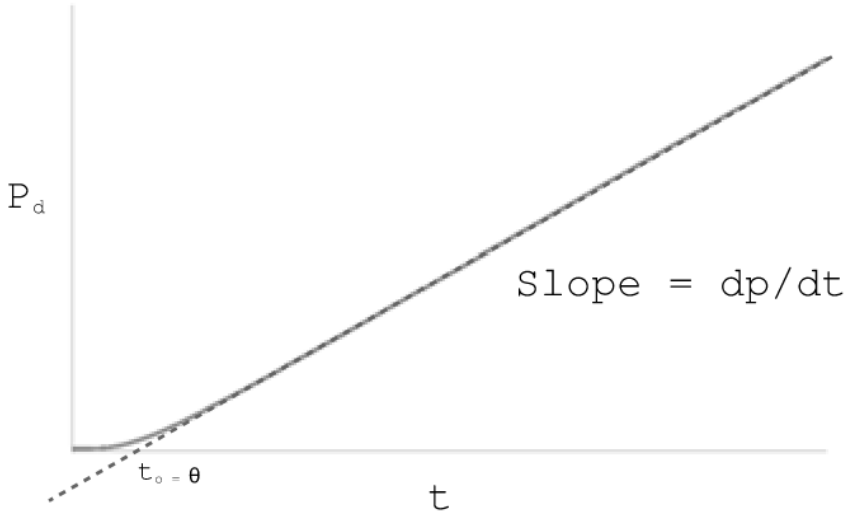

Figure 3-2: Typical progress of a dynamic gas permeation test in a CV system.

By obtaining the slope from the pressure response curve, Equation 3.3 can be used to obtain the permeation rate (Q).

The pressure response can be modelled by first starting with the continuity equation (3.4) and Fick's first law (3.5), shown below [4].

$$\frac{\partial C}{\partial t} = -\frac{\partial J}{\partial x} \qquad 3.4$$

$$J = -D\frac{\partial C}{\partial x} \qquad 3.5$$

Taking the derivative of equation 3.5 and substituting it into equation 3.4 results in equation 3.6 below, which is Fick's second law of diffusion.

$$\frac{\partial C}{\partial t} = D\frac{\partial^2 C}{\partial x^2} \qquad 3.6$$

The initial and boundary conditions for the ideal time lag experiment are as follows:

1. The concentration at any point in the membrane is equal to zero at time zero (the membrane is completely degassed, i.e. initial condition C(x,0) = 0.
2. The concentration at the membrane surface that is exposed to the pressurized gas follows Henry's law, i.e. boundary condition C(0,t) = Sp_o, where p_o is constant, i.e. the first boundary condition), and,
3. The concentration at the membrane surface exposed to vacuum is zero, i.e. boundary condition C(L,t) = 0.

Equation 3.6 can be solved using the separation of variables to obtain equation 3.6 below.

$$C(x,t) = \frac{p_0 P}{D}\left(1 - \frac{x}{L}\right) - 2\frac{p_0}{\pi D}\left[\sum_{n=1}^{\infty}\frac{1}{n}sin\left(\frac{n\pi x}{L}\right)exp\left(-\frac{Dn^2\pi^2 t}{L^2}\right)\right] \qquad 3.7$$

Applying Fick's first law (Equation 3.5) to Equation 3.7 and evaluating it at x = L will produce Equation 3.8. This is the molar gas flux leaving the membrane.

$$J(x = L, t) = \frac{p_0 P}{L} + \frac{2p_0 P}{L}\left[\sum_{n=1}^{\infty}(-1)^n exp\left(-\frac{Dn^2\pi^2 t}{L^2}\right)\right] \qquad 3.8$$

Multiplying the molar flux [mol/s-m^2] shown in Equation 3.7 by the area of the membrane provides the molar flow entering the downstream receiver (at x=L) at the time, t. Assuming the ideal gas law holds at these low pressures, the molar flow can be multiplied by RT/V (ideal gas constant, temperature and receiver volume) and integrated over time. This allows for determining the pressure rise as a function of time [Pa/s], shown in Equation 3.8. The variables in Equation 3.8 are as follows: pressure step change, p_o, membrane area, A, the system's absolute temperature, T, the volume of the receiver, V, membrane thickness, L and the volume of one mole of gas at STP conditions, v_{STP}.

$$p(t) = \frac{Ap_0PRT}{Vv_{STP}L}\left[t - \frac{L^2}{6D} + \frac{2L^2}{\pi^2 D}\sum_{1}^{\infty}\frac{(-1)^{n+1}}{n^2}\exp(-n^2 Fo \cdot \pi^2)\right] \quad 3.9$$

Equation 3.9 covers the transient and steady-state behaviour of the pressure response. As the time approaches infinity, the mass Fourier number grows larger, and the exponential term approaches zero. The mass Fourier number, defined in equation 3.10, is analogous to the Fourier number, which is a dimensionless time that characterizes transient heat conduction. As Fo increases, i.e. steady-state conditions are attained, the summation term disappears and Eq. 3.9 becomes equation 3.11.

$$Fo = \frac{Dt}{L^2} \quad 3.10$$

$$p(t) = \frac{Ap_0PRT}{Vv_{STP}L}\left[t - \frac{L^2}{6D}\right] \quad 3.11$$

The x-intercept of the linear portion of pressure response with the time axis, i.e. for p = 0, is the time lag (Θ) and is equal to:

$$t = \theta = \frac{L^2}{6D} \quad 3.12$$

Once this time lag is determined, the diffusivity can be calculated if the membrane thickness is known. The slope of the linear portion, i.e. dp/dt is shown in Equation 3.13 and can be used to find the permeability (P). A time-lag experiment is presented in Figure 3-3, where nitrogen is permeating through a Poly(2,6-dimethyl-1,4-phenylene oxide) (PPO) membrane at 194 Torr and 30℃.

$$P = \frac{\left(\frac{dp}{dt}\right)Vv_{STP}L}{Ap_0RT} \quad 3.13$$

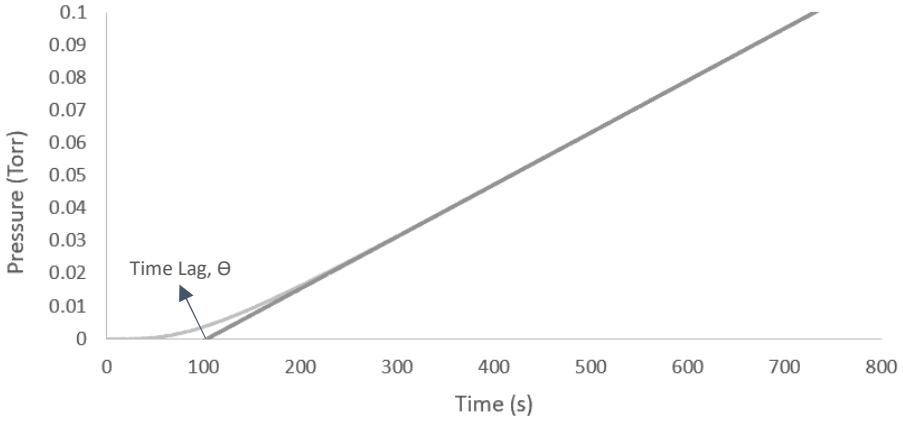

Figure 3-3: The traditional time-lag experiment –nitrogen permeating through a PPO membrane at 194 Torr and 30℃.

From the diffusivity and permeability calculated earlier, the solubility can be obtained using Equation 3.1.

3.2 Novel Time-Lag Experiments for Determining Membrane Properties

As discussed in section 3.1.3, the time lag experiment is usually done using a single-step change from vacuum conditions to a new pressure p_o. However, in reality, additional parameters such as the saturation and affinity constants, the diffusivity coefficient related to the Langmuir sites and the equilibrium constant between the Henry's and Langmuir sites need to be determined as well[10]. Henry's law on its own is not applicable due to the two modes of sorption that occurs in glassy polymers – the dual sorption model assumes that a polymer consists of a continuous chain matrix, along with microvoids (holes), frozen in the matrix [10]. The dual sorption is then defined in terms of Henry's law of solubility (dissolution in continuous chain matrix) and Langmuir-type of sorption (sorption in microvoids)[10]. These parameters are found by completing multiple time-lag experiments at different pressures. It is important to note that Henry's law applies to rubbery polymers for low molecular weight gases and at low gas pressures [10].

A novel method of determining these properties is proposed. Instead of a single step change from vacuum conditions to a new pressure, a series of step changes is completed during the same experiment. As a result, the concentration profile of the membrane at time zero is no longer equal to zero. It will be the steady-state concentration profile from the previous step.

This chapter aims to demonstrate that multiple dynamic time lag experiments can be performed in a single, combined experiment. The membrane material of interest is PPO, a glassy polymeric material of broad interest in gas separation applications due to its high permeability and moderate selectivity[11]. It is well known that the properties of glassy polymers, such as PPO, vary with feed pressure [3,10]; therefore, the direct comparison of the properties obtained using the experimental protocol below is not the intention.

3.2.1 Experimental Procedure and Materials

The system used for the permeation experiments in this chapter is a constant volume system which is shown in Figure 3-4. Additional valves and volumes that were not used for these experiments were left out of the figure for simplification.

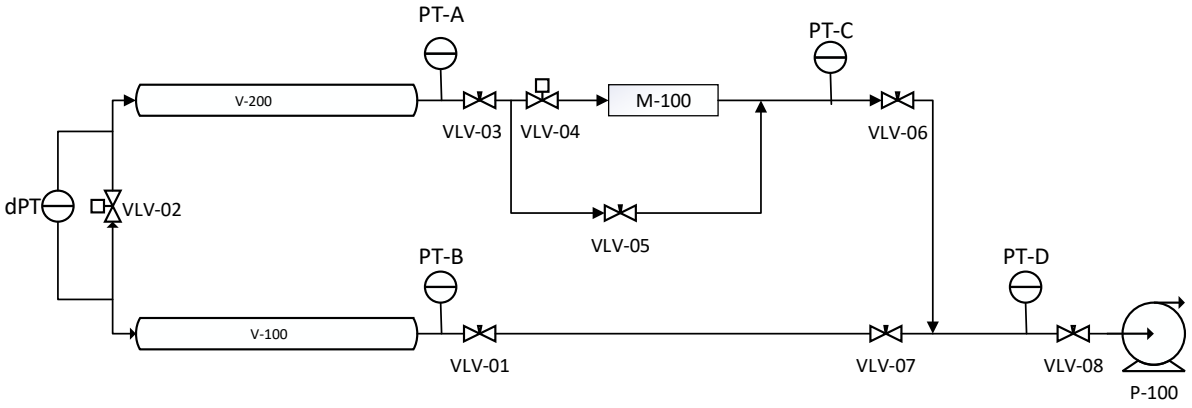

Figure 3-4: Experimental setup

Table 3-1: Equipment legend

Tag	Description
dPT	Differential pressure transmitter
PT-A	Absolute pressure transmitter A
PT-B	Absolute pressure transmitter B
PT-C	Absolute pressure transmitter C
PT-D	Absolute pressure transmitter D
M-100	Membrane cell
P-100	Vacuum pump
VLV-02, VLV-04	Actuated valves
VLV-01,VLV-03,VLV-05,VLV-06,VLV-07	Manual valves
V-100	Reference volume
V-200	Working volume

To create the membrane, PPO was dissolved in chloroform to produce a 10-weight % solution of PPO. The membrane was spin-coated three times over a silicon wafer to form a thickness of 80 microns. This was done over a year ago, and the membrane was stored in a dry, enclosed location. The differential pressure transducer provides the difference in pressure between the working and reference volumes and has a range of 1 Torr. This is especially useful when performing upstream pressure decay experiments when the pressure drop is minuscule. The absolute pressure transmitters, of course, measure the absolute pressure at the locations of interest- at the working and reference volumes and downstream of the membrane. PT-A and PT-B have a range of 2000 Torr, while PT-C and PT-D have a range of 10 Torr. The receiving volume is the tubing that extends from downstream of the membrane to VLV-08. This volume is estimated to be 65 cm^3. The reference and working volumes are equal in size; they are 115.1 cm^3. The valves, of course, allow for the isolation of the volumes, membrane, pump, etc.

Two types of experiments were conducted: a step-up experiment and a step-down one. To complete a step-down experiment, the reference and working volumes, V-200 and V-100 in Figure 3-4, are filled with nitrogen to a pressure, P_1. The membrane, M-100, is degassed for at least 24 hours to ensure no concentration profile across the membrane and that the receiving volume is a vacuum. The reference and working volume are isolated at pressure P_1, and the experiment is started by opening the valves

between the working volume and membrane cell. The pressure rise downstream is monitored, and after a steady state is reached, the reference volume is purged to a pressure, P_2, that is lower than P_1, and the valve between the two volumes is opened to cause a sudden pressure drop in the working volume. The two volumes are then isolated once again, and the system is allowed to reach a steady state at the lower feed pressure. The procedure is repeated until the pressure transmitter on the receiving volume reaches its upper limit (10 torr). The step-up experiment is identical to the step-down experiment, except the reference volume is pressurized to a higher pressure than the previous step. Once the valve between the reference and working volume is opened, the working volume experiences a sudden increase in pressure. It is important to note that leak tests were done to ensure that the system was not taking on gas. Since the system is at a high vacuum, a leak would result in pressurization downstream of the membrane cell. It was deemed that the rate of pressure rise due to micro leaks was negligible.

3.2.1.1 Properties of PPO Membrane

The transport properties of PPO membranes depend on the degree of crystallinity, which depends on the type of PPO powder that is used[12]. In work done by Alentiev et al., three PPO powders of varying crystallinity and molecular weight were tested. These membranes were designated as PPO-1 (M_W=636 kDa), PPO-2 (M_W=355 kDa) and PPO-4(M_W=610 kDa). The mentioned PPO films (PPO-1, PPO-2, and PPO-4) were prepared by casting the solution in chloroform (5 wt%) on cellophane support and drying at room temperature for 2–3 days[12]. Another PPO-2 membrane was produced, but this time the membrane was dried on a heated table at 50°C. The permeability, diffusivity and solubility are summarized in Table 3-2 below.

Table 3-2: Properties of PPO membranes of varying crystallinity [12]

Membrane Properties (30°C)	**PPO-2-50°C (M_W=355 kDa)**	**PPO-2 (M_W=355 kDa)**	**PPO-1 (M_W=636 kDa)**	**PPO-4(M_W=610 kDa)**
Permeability, P (Barrer)	2.5 ± 0.1	7.1 ± 0.4	9.0 ± 0.4	14.0 ± 0.7
Diffusivity, D (cm^2/s)	(3.6 ± 0.4) $x10^{-8}$	(5.5 ± 0.6) $x10^{-8}$	(7.5 ± 0.8) $x10^{-8}$	(10 ± 1) $x10^{-8}$
Solubility, S (cm^3 (STP)/(cm^3·cmHg)	(7.0 ± 1.0) $x10^{-3}$	(13 ± 2) $x10^{-3}$	(12 ± 2) $x10^{-3}$	(14 ± 2) $x10^{-3}$

3.2.2 Mathematical Interpretation of the Experiment

The following analysis applies to rubbery polymers; as stated earlier, PPO is a glassy polymer, so the apparent diffusivity will depend on feed pressure. Further work is being done by others to determine if this apparent diffusivity is statistically significant. For this chapter, the apparent diffusivity is assumed to be constant in each step. When the feed pressure changes, the new equilibrium concentration at the feed face of the membrane is assumed to be established instantaneously. Consequently, a step change in the feed pressure from p_0 to p_1 leads to a step change in the equilibrium concentration at the feed face of the membrane from C_0 to C_1[3].This is a key assumption of the solution-diffusion model. Once again, starting

from the continuity equation and Fick's first law (Equations 3.4 and 3.5), Equation 3.6 is obtained, but this time with new initial/boundary conditions.

Since steady-state permeation is already occurring across the membrane, there is a linear concentration gradient across the membrane thickness. Equation 3.14, which is the initial condition, represents this concentration gradient:

$$C(x, t = 0) = C_0 - (C_0 - C_L)\frac{x}{L} \qquad 3.14$$

The two boundary conditions required for the solution of equation 3.5 are given by the following equations,

$$C(x = 0, t > 0) = C_1 \qquad 3.15$$

$$C(x = L, t) = C_L \qquad 3.16$$

Lashkari et al. solved Equation (3.6) by the method of separation of variables, which results in equation 3.17, shown below.

$$C = C_1 - (C_1 - C_L)\frac{x}{L} - \frac{2(C_1 - C_0)}{\pi}\sum_{n=1}^{\infty}\frac{1}{n}sin\left(\frac{n\pi x}{L}\right)exp\left(-n^2\pi^2\frac{Dt}{L^2}\right) \qquad 3.17$$

Differentiating Equation 3.17 with respect to x and multiplying by the constant membrane diffusivity results in Equation 3.18 below.

$$J(x, t) = D\frac{(C_1 - C_L)}{L} + 2D\frac{(C_1 - C_0)}{L}\sum_{n=1}^{\infty}cos\left(\frac{n\pi x}{L}\right)exp\left(-n^2\pi^2\frac{Dt}{L^2}\right) \qquad 3.18$$

Setting x = L provides the final expression for the transient gas flux leaving the membrane and is shown in Equation 3.19

$$J(L, t) = D\frac{(C_1 - C_L)}{L} + 2D\frac{(C_1 - C_0)}{L}\sum_{n=1}^{\infty}(-1)^n exp\left(-n^2\pi^2\frac{Dt}{L^2}\right) \qquad 3.19$$

To obtain an expression for the rate of pressure increase in the receiving volume, equation 3.19 is multiplied by the area, ideal gas constant, and temperature and divided by the volume, followed by integration from zero to time "t." This results in equation 3.20 shown below:

$$p(t) = \frac{ART}{V}\left[D\frac{C_1}{L}t - \frac{L(C_1 - C_0)}{6} - 2\frac{L(C_1 - C_0)}{\pi^2}\sum_{n=1}^{\infty}\frac{(-1)^n}{n^2}\exp(-n^2\pi^2 Fo)\right] \qquad 3.20$$

Equation 3.19 represents the transient pressure response; however, as the time approaches infinity, this equation can be simplified into Equation 3.21, i.e. the rate of pressure rise at a steady state.

$$p(t) = \frac{ART}{V}\left(D\frac{C_1}{L}t - \frac{L(C_1 - C_0)}{6}\right) \qquad 3.21$$

3.2.3 Experimental Results and Discussion

3.2.3.1 Step-Up Experiment

The membrane cell and all downstream tubing were evacuated for 24 hours with a vacuum pump to ensure near-vacuum conditions (approximately 10^{-4} Torr). The working and reference volumes were pressurized to 875 Torr and were allowed to reach a temperature of 30°C. The working and reference volumes were then isolated, and the membrane cell was exposed to the working pressure. After approximately 1.25 hours, the system was deemed to have reached a steady state for a sufficient amount of time, and the pressure step increase was initiated. The reference volume was pressurized to about 1475 Torr, and the valve isolating the working and reference volume was suddenly opened and closed. This caused the pressure in the working and reference volume to equilibrate at 1210 Torr, which was the new feed pressure to the membrane. The system took approximately 1.25 hours to reach a steady state, and the protocol was repeated for the pressure of 1650 Torr.

Figure 3-5 shows the results of the step-up experiment. It can be seen that the rate of pressure rise increases as the feed pressure increases. There is a gradual increase in the permeation rate until a new steady state is reached. The slopes of the linear regions and the x-intercepts (time lag) are summarized in Table 3-2 below. A simple check to ensure the experiment was successful was to compare the pressure increase factor (i.e. the ratio of the new/old pressure) to the slope increase factor (i.e. the ratio of the new/old slopes). They were within 2% of each other, indicating that the pressure rise/decrease rate was linearly proportional to the feed pressure, as expected.

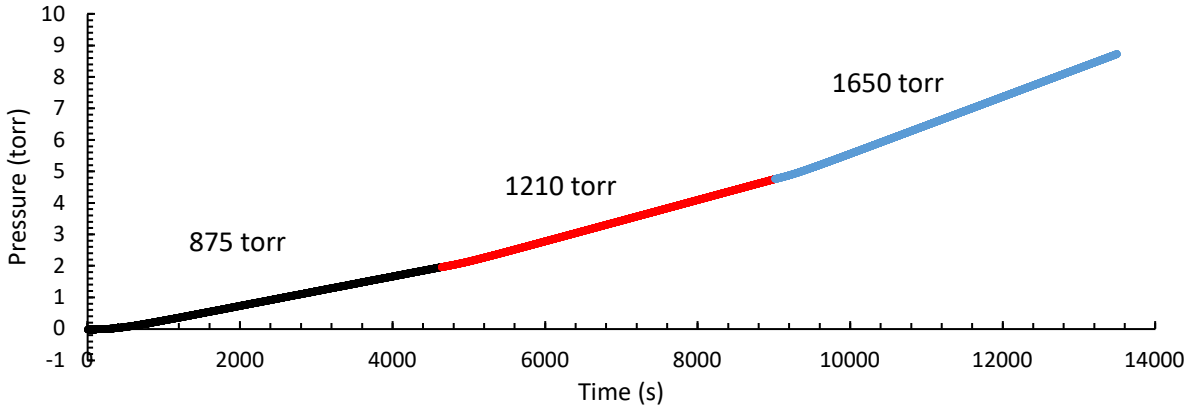

Figure 3-5: Results from the "Step-up" permeation experiment. This figure shows the rate of pressure rise at three feed pressures – 875 Torr, 1210 Torr and 1650 Torr. The change in feed pressure occurs when the previous experiment reaches a steady state.

The data from Figure 3-5 can be further analyzed to obtain the traditional time-lag plots shown in Figure 3-6. First, a line of best fit is determined from the linear portion of the transient response. This is done

using the Excel line estimation function, and the slopes for each step are shown in Table 3-3. The 1210 Torr and 1650 Torr step changes are then normalized by subtracting the steady state permeation from the previous step from the pressure response. The experimental time is reset to zero seconds for each subsequent step.

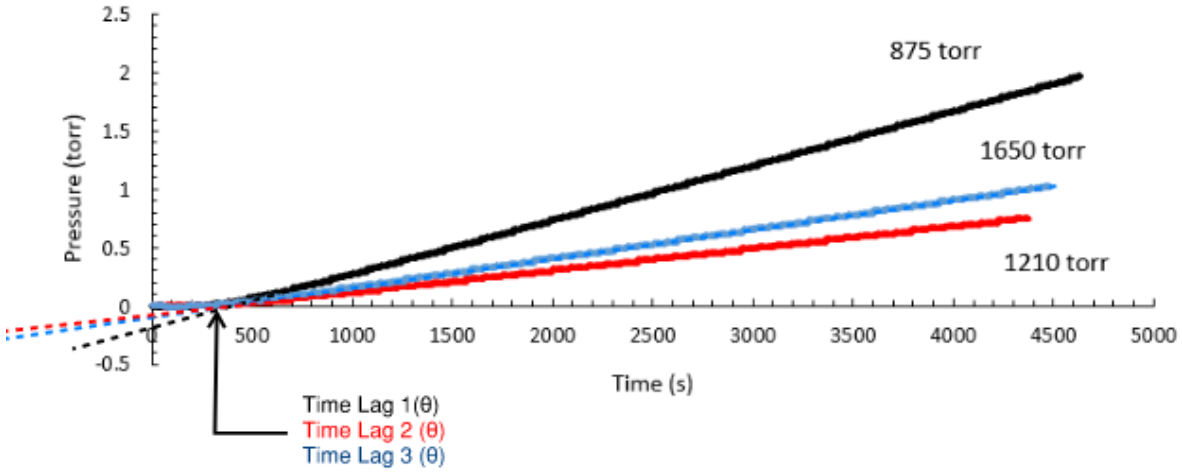

Figure 3-6: Normalized pressure responses and lines of best fit to show the experimental time lags from the step-up experiment.

Table 3-3: Summary of the step-up experiment results

Feed Pressure (Torr)	Slope (Torr/s)	Time Lag (s)	Slope Increase Factor	Pressure Increase Factor
875	0.000467	423	--	--
1210	0.000656	405	1.405	1.382
1650	0.000250	374	1.381	1.363

Note 1: The slope is obtained from the original data, i.e. Figure 3-5.
Note 2: The time lags are obtained from the normalized data, i.e. Figure 3-6.

The time lags were obtained within 13% of each other – the average time lag was found to be 402s with a standard deviation of 22s. This means that the resulting calculated effective diffusivities would be within 13% of each other, which is not a significant difference and may be due to the glassy nature of the PPO membrane. It is important to note that the first step of the permeation experiment has a different initial condition compared to the subsequent steps. The difference is that the concentration in the membrane in the first step is near zero, while in the subsequent steps, there is a linear concentration profile in the membrane. This is the primary source of the transient behaviour that results in different time lags when comparing the first step to the subsequent steps. The difference in the time lag between the first and last steps, for example, is approximately 13%; however, the difference between the second and third steps is only 8%. This transient behaviour will be discussed further in the step-down experiment.

From the resulting time-lags, the effective membrane diffusivity is obtained using Equation 3.12 and shown in Table 3-3. The membrane thickness was measured to be approximately 80 microns, which is

required to perform the calculations displayed in the previous section. From the resulting slopes, the permeability can be obtained using equation 3.11. The volume of the receiver was measured to be 85 $cm^{3,}$ and the temperature of the system was set to 30°C. The membrane area was calculated to be about 11.4 cm^2. The ideal gas constant, step pressure and molar volume are known; therefore, the permeability is calculated and shown in Table 3-4. From the permeability and diffusivity, the solubility is calculated using Equation 3.1.

Table 3-4: Summary of calculated membrane properties for step-up experiment.

Feed Pressure (Torr)	Diffusivity (cm^2/s)	Permeability (Barrer)	Solubility $cm^3(STP)/(cm^3$ x cmHg)
875	$2.50x10^{-8}$	3.77	$1.51x10^{-2}$
1210	$2.63x10^{-8}$	3.83	$1.45x10^{-2}$
1650	$2.86x10^{-8}$	3.88	$1.36x10^{-2}$

3.2.3.2 Step-Down Experiment

The experimental protocol specified in 3.3.4.1 was modified where the experiment begins at the highest pressure and steps down. As always, the membrane cell and receiving volume were evacuated with the turbo-molecular pump to near vacuum conditions. The reference and working volume were pressurized to 1755 Torr and were isolated from each other. The valve between the membrane cell and the working volume was opened, which initiated the experiment. The system reached a steady state after approximately 1.25 hours, and the reference volume was evacuated to prepare for the step-down. The valve between the working and reference volume is opened and immediately closed, which results in an immediate expansion of the working volume and a decrease in pressure to approximately 1317 Torr. This procedure was then repeated to achieve a working pressure of 952 Torr. The results of this experiment can be seen in Figure 3-7 below.

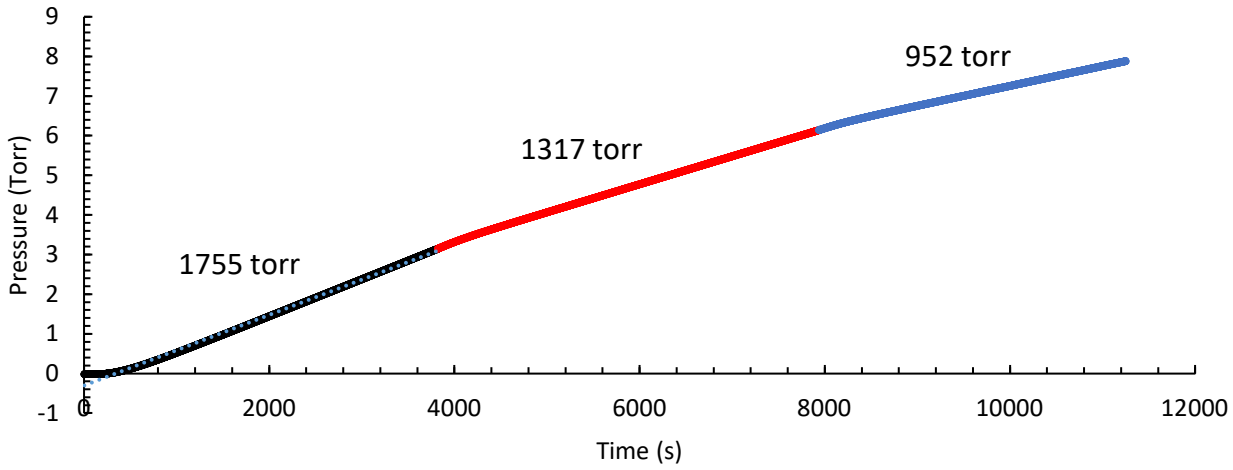

Figure 3-7: Results of the step-down permeation experiment. This figure shows the rate of pressure rise at three feed pressures – 1755 Torr, 1317 Torr and 952 Torr. The change in feed pressure occurs when the previous experiment reaches a steady state.

It can be seen that the rate of pressure rise decreases as the feed pressure increases, which is an expected result. There appears to be a smooth transition from one steady-state permeation rate to the next. Similarly to the step-up experiment, further analysis is done to normalize the curves and obtain time lags for each step, which is shown in Figure 3-9 and Table 3-5. The time lag for the initial permeation experiment, i.e. a, from vacuum conditions to 1755 torr, shows a time lag of 448 seconds, while the time lag obtained from the steady state initial conditions shows time lags of 359s and 371s for 1317 torr and 952 torrs respectively. The average time lag was calculated to be 392 s with a standard deviation of 40 s.

The difference in time lag for the second and third steps was much lower (~3%) compared to the difference between the first and second steps (20%) or the first and last steps (17%). This can be attributed to the glassy nature of PPO, resulting in pressure-dependent effective diffusivity. In addition to this, when a linear concentration profile exists at higher working pressure, a sudden decrease in working pressure will result in diffusion in two directions. This can be shown in Figure 3-8 below. Until the membrane reaches a new linear concentration profile, based on the new pressure, there exists a short time where diffusion will occur in both directions since both faces of the membrane are at a concentration lower than at a position within the membrane.

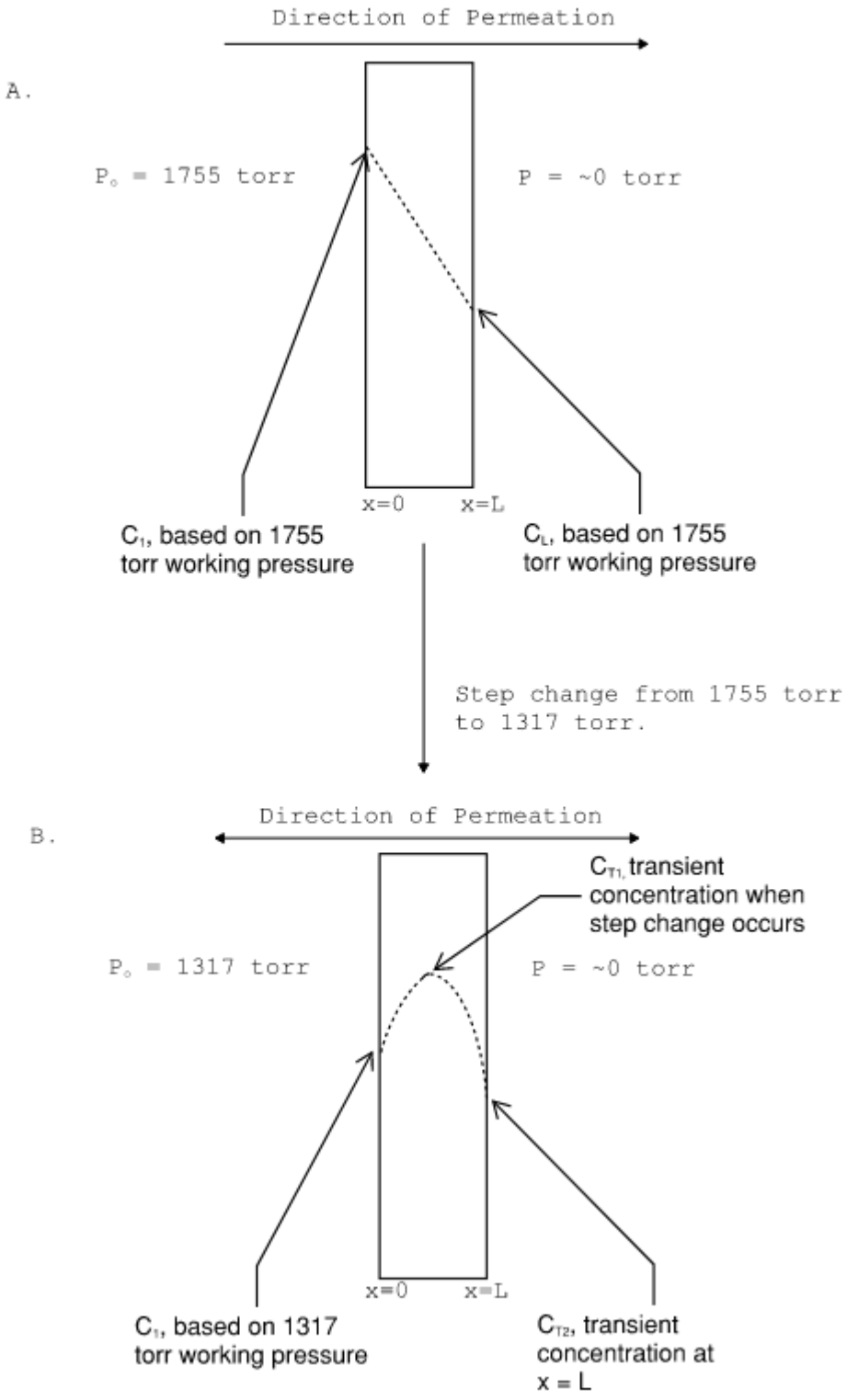

Figure 3-8: Steady state (A) and transient (B) concentration profiles.

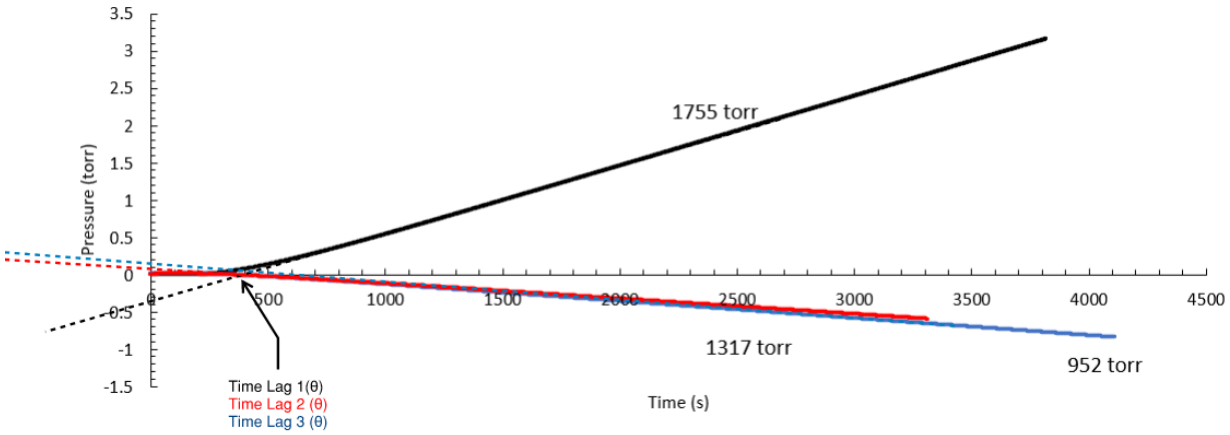

Figure 3-9: Normalized pressure responses and lines of best fit to show the experimental time lags from the step-down experiment.

Table 3-5: Summary of the step-down experiment results

Feed Pressure (Torr)	Slope (Torr/s) (Note 1)	Time Lag (s) (Note 2)	Slope Decrease Factor	Pressure Decrease Factor
1755	0.000934	448	--	--
1317	0.000707	359	0.76	0.75
952	0.000502	371	0.71	0.72

Note 1: The slope is obtained from the original data, i.e. Figure 3-7.
Note 2: The time lags are obtained from the normalized data, i.e. Figure 3-4.

Similarly to the step-up experiments, the membrane properties can be calculated knowing the thickness of the membrane, the membrane area and the receiver volume. These properties are summarized in Table 3-6 below.

Table 3-6 Summary of calculated membrane properties for the step-down experiment.

Feed Pressure (Torr)	Diffusivity (cm^2/s)	Permeability (Barrer)	Solubility $cm^3(STP)/(cm^3 \times cmHg)$
1755	2.38×10^{-8}	3.76	1.58×10^{-2}
1317	2.97×10^{-8}	3.80	1.28×10^{-2}
952	2.87×10^{-8}	3.84	1.34×10^{-2}

Table 3-7 below summarizes the average membrane properties found from the step-up and step-down experiments. The permeabilities, diffusivities and solubilities obtained from these experiments are within the range found in the literature, which is shown in Table 3-2.

Table 3-7: Average membrane properties obtained from both the step-up and step-down procedure

Experiment	Diffusivity (cm^2/s)	Permeability (Barrer)	Solubility cm3(STP)/(cm3 x cmHg)
Step-Up Experiment	$2.66x10^{-8}$	3.83	$1.44x10^{-2}$
Step-Down Experiment	$2.74x10^{-8}$	3.80	$1.40x10^{-2}$

3.2.3.3 The Glassy Nature of PPO

As stated earlier, the conventional time-lag analysis is limited to membranes in which gas sorption follows Henry's law, i.e. to rubbery membranes[13]. Due to the fact that the PPO membrane is a glassy polymer, gas sorption does not follow a linear isotherm, i.e. S is not constant but depends on the gas concentration in the membrane[13]. This could be part of the reason why the diffusivities and, therefore, solubilities do not match the values seen in the literature and are lower by order of magnitude. The dual-mode sorption model that is applicable to glassy polymers and should be used in future work can be found in Equation 3.22 below[13].

$$C = C_D + C_H = S_P + \frac{C'_H bp}{1 + bp} \qquad 3.22$$

where C_D and C_H refer to the gas concentrations in Henry's and Langmuir's sites, respectively, p is the gas pressure in contact with the membrane, and C'_H and b are the hole saturation and the hole affinity constants, respectively.

Glassy polymers are in a nonequilibrium thermodynamic state at temperatures below their T_g, and as a result, they experience physical aging as they approach equilibrium[14]. This process is typically characterized by changes in properties like volume, enthalpy, entropy, etc. Most importantly, it has been reported that aging affects the free volume of glassy polymers. As a result, the permeability, diffusivity and solubility change with aging time[14]. Understanding this aspect of physical aging is of considerable importance for membrane technology since polymeric membranes used in industrial applications may degrade in performance just after a few years of service. Although the properties of the PPO membrane were within the range found in literature, physical aging could have changed these properties. Future work should be done to test the membrane soon after production, followed by regular intervals to quantify the reduction in performance.

3.3 Conclusion

Performing time-lag experiments step-wise is an alternative to evacuating the system after each permeation experiment and restarting at a new working pressure. The time lags obtained and the calculated membrane properties are within 13% and 20% of each other for the step-up and step-down experiments, respectively. Because the initial condition for the first step is a near-zero concentration in the membrane, and the initial conditions for the subsequent steps are linear concentration profiles, the second and third steps behave more similarly compared to the first step. This should also result in closer membrane properties calculated for the second and third steps compared to the first, which is shown in the results of the step-down experiment. The average diffusivity obtained from the step-up procedure was 2.66 $x10^{-8}$ cm^2/s, the average permeability was 3.83 Barrer, and the average solubility was $1.44x10^{-2}$ $cm^3(STP)/(cm^3$ x cmHg). From the step-down experiments, the average diffusivity was $2.74x10^{-8}$ cm^2/s, the

average permeability was 3.80 Barrer, and the average solubility was 1.40×10^{-2} cm3(STP)/(cm^3 x cmHg). The slight deviation in diffusivity at the various feed pressures could arise from the glassy nature of the PPO membrane, which results in pressure-dependent diffusion coefficients as opposed to rubbery polymers. The deviation in the time lag and, therefore, diffusivity between the first step and the subsequent steps could be a result of the transient concentration profile within the membrane when the working pressure is decreased, which results in some back diffusion. When the working pressure is increased, back diffusion does not occur, but it is expected that another transient phenomenon will occur, which may cause unexpected results. The difference in diffusivity and solubility between the experimental values and the ones obtained in literature could be a result of the physical aging of the glassy membrane.

3.4 Recommendations

More work should be done to analyze the transient behaviour during the steady state step changes. In order to accomplish this, a thicker membrane can be used or a larger receiving volume (cylindrical vessels are available downstream of the membrane cell) to allow for a higher number of steps per experiment. The bottleneck as of this moment is the pressure range of the downstream pressure transmitters (10 Torr). In addition, the magnitude of the pressure step change should be increased; for example, the first step could be 200 Torr, followed by a single subsequent step to 2000 Torr. The experiments should also be repeated at various temperatures to determine if the transient behaviour is more or less visible.

Work should be done to determine if the apparent diffusivities that result from the glassy nature of the PPO membrane are statistically significant or if the slight differences are purely a result of transient behaviour, temperature effects, etc. Further experiments can be carried out where the step-ups and step-downs are combined into a single experiment. This method will begin with a small step-up, and once a steady state is reached, another 2-3 free step-ups are performed. From there, 2-3 step-downs would be performed at similar pressures that were used on the way up. This procedure allows for a simpler comparison of the step-up and step-down experiments. Lastly, work should be done to test the membrane at various intervals to quantify the effects of physical aging.

References

[1] M. Mulder, Basic principles of membrane technology, 2nd ed., Dordrecht ; Boston : Kluwer Academic, 1996.

[2] M. Farnam, H. bin Mukhtar, A. bin Mohd Shariff, A Review on Glassy and Rubbery Polymeric Membranes for Natural Gas Purification, ChemBioEng Reviews. 8 (2021) 90–109. https://doi.org/10.1002/cben.202100002.

[3] S. Lishkari, B. Kruczek, Membrane Characterization Using the Time Lag Method in a Constant Volume System, (n.d.).

[4] R.W. Baker, Membrane Technology and Applications, John Wiley & Sons, Ltd., 2012.

[5] M. Farnam, H. Mukhtar, A.M. Shariff, A review on glassy polymeric membranes for gas separation, in: Applied Mechanics and Materials, Trans Tech Publications Ltd, 2014: pp. 701–703. https://doi.org/10.4028/www.scientific.net/AMM.625.701.

[6] S. Lashkari, A. Tran, B. Kruczek, Effect of back diffusion and back permeation of air on membrane characterization in constant pressure system, J Memb Sci. 324 (2008) 162–172. https://doi.org/10.1016/j.memsci.2008.07.006.

[7] B. Kruczek, S. Lashkari, Challenges in Microflow Measurements, (2012).

[8] G.L. Morini, Y. Yang, H. Chalabi, M. Lorenzini, A critical review of the measurement techniques for the analysis of gas microflows through microchannels, Exp Therm Fluid Sci. 35 (2011) 849–865. https://doi.org/10.1016/j.expthermflusci.2011.02.005.

[9] B. Kruczek, CHG 8194 Membrane Separation Processes - Membrane Characterization, n.d.

[10] Chapter 4. Permeability, Diffusivity, and Solubility of Gas and Solute Through Polymers, n.d.

[11] R. Rea, S. Ligi, M. Christian, V. Morandi, M.G. Baschetti, M.G. de Angelis, Permeability and selectivity of PPO/graphene composites as mixed matrix membranes for CO2 capture and gas separation, Polymers (Basel). 10 (2018). https://doi.org/10.3390/polym10020129.

[12] A.Y. Alentiev, I.S. Levin, N.A. Belov, R.Y. Nikiforov, S. v. Chirkov, D.A. Bezgin, V.E. Ryzhikh, J. v. Kostina, V.P. Shantarovich, L.Y. Grunin, Features of the gas-permeable crystalline phase of poly-2,6-dimethylphenylene oxide, Polymers (Basel). 14 (2022). https://doi.org/10.3390/polym14010120.

[13] N. Al-Qasas, J. Thibault, B. Kruczek, A new characterization method of membranes with nonlinear sorption isotherm systems based on continuous upstream and downstream time-lag measurements, J Memb Sci. 542 (2017) 91–101. https://doi.org/10.1016/j.memsci.2017.07.039.

[14] Y. Huang, D.R. Paul, Experimental methods for tracking physical aging of thin glassy polymer films by gas permeation, J Memb Sci. 244 (2004) 167–178. https://doi.org/10.1016/j.memsci.2004.06.058.

Chapter 4. Overall Conclusions and Recommendations

4.1 Testing and Data Analysis of Water Miscible Flammable Liquid Mixtures

The flash and fire point of the water-miscible flammable liquids (methanol, ethanol, 2-propanol, acetone and acetic acid) were higher when mixed with water. Of course, as the water concentration increased, the flash and fire points also increased due to the lower partial pressure of flammable vapours above the liquid and the higher partial pressure of the non-flammable species (water) in the vapour phase. At high enough water concentrations (usually above 90%), a flash/fire point was never observed for every WMFL mixture, excluding acetone water– the amount of vapour produced would not reach the LFL. As a result, the fire safety risk of WMFLs is much lower than their pure species counterparts. In the National Fire Code/Building Code of Canada, WMFL mixtures should not be in the same category as pure species. Their regulations should be less stringent. Using an automated, closed-cup instrument for binary mixtures is recommended, or a modified version of the ASTM standard to reduce the composition and liquid level variation as the experiment progresses.

4.2 Novel Methods of Membrane Characterization Using Steady State Step Changes

The novel time-lag determination involved performing step changes in pressure while steady-state permeation was already occurring in the membrane. This method allows for determining multiple time lags at varying feed pressures in a single experimental procedure. For both the step-up and step-down pressure tests, the resulting time lags were within 20% and 13% of each other, respectively. However, this difference was smaller for the second and third steps, where the initial conditions for both experiments were the same. Using this membrane characterization method, the average diffusivity obtained from the step-up procedure was 2.66×10^{-8} cm^2/s, the average permeability was 3.83 Barrer, and the average solubility was 1.44×10^{-2} $cm^3(STP)/(cm^3 \times cmHg)$. From the step-down experiments, the average diffusivity was 2.74×10^{-8} cm^2/s, the average permeability was 3.80 Barrer, and the average solubility was 1.40×10^{-2} $cm3(STP)/(cm^3 \times cmHg)$. It is recommended to further analyze the transient behaviour – this can be done by performing more pressure steps in the same experiment, using a thicker membrane or larger receiving volume. In addition, the magnitude of the pressure step change could be increased, and the number of steps decreased; for example, the first step could be 200 Torr, followed by a single subsequent step to 2000 Torr. The experiments should also be repeated at various temperatures to determine if the transient behaviour is more or less visible. Future work should be done to determine if the deviation in membrane properties at the various feed pressures was partly a result of the glassy nature of the PPO membrane. Work should be done to test the membrane at various intervals to quantify the effects of physical aging.

Appendix A – Raw Data Tables for Chapter 2

Table A-1: Boiling point of Methanol-Water mixture at various concentrations (3 replicates and their average values)

Methanol (% vol.)	Boiling point of mixture (°C)		Average boiling point of mixture (°C)	Observation
90	1	68.00± 0.01	68.67± 0.01	-
	2	68.28± 0.01		-
	3	69.74± 0.01		-
80	1	71.39± 0.01	71.78± 0.01	-
	2	71.43± 0.01		-
	3	72.52± 0.01		-
70	1	73.54± 0.01	73.95± 0.01	-
	2	73.55± 0.01		-
	3	74.78± 0.01		-
60	1	76.77± 0.01	76.52± 0.01	-
	2	77.00± 0.01		-
	3	75.79± 0.01		-
50*	1	78.91± 0.01	79.02± 0.01	-
	2	79.10± 0.01		-
	3	79.05± 0.01		-
40*	1	81.71± 0.01	81.73± 0.01	-
	2	81.71± 0.01		-
	3	81.77± 0.01		-
30	1	84.49± 0.01	84.50± 0.01	-
	2	84.75± 0.01		-
	3	84.27± 0.01		-
20	1	88.49± 0.01	88.69± 0.01	-
	2	88.58± 0.01		-
	3	89.00± 0.01		-
10	1	93.77± 0.01	94.19± 0.01	-
	2	94.11± 0.01		-
	3	94.71± 0.01		-
5	1	97.02± 0.01	97.22± 0.01	-
	2	97.64± 0.01		-
	3	97.00± 0.01		-

* Additional tested Methanol concentrations

Table A-2: Average boiling points of Methanol-Water mixture at various concentrations and 2 commercial products

Methanol (% vol.)	Average boiling point of mixture (°C)	Average boiling point of commercial product (°C)
90	68.67± 0.01	-
80	71.78± 0.01	-
70	73.95± 0.01	-
60	76.52± 0.01	-
50*	79.02± 0.01	78.51± 0.01†
40*	81.73± 0.01	80.63± 0.01‡
30	84.50± 0.01	-
20	88.69± 0.01	-
10	94.19± 0.01	-
5	97.22± 0.01	-

* Additional tested Methanol concentrations
† Reflex Windshield Washer Fluid, -49 °C
‡ Certified Windshield Washer Fluid, -35 °C

Table A-3: Boiling point of Ethanol-Water mixture at various concentrations (3 replicates and their average values)

Ethanol (% vol.)		Boiling point of mixture (°C)	Average boiling point of mixture (°C)	Observation
90	1	79.65± 0.01	79.58± 0.01	-
	2	79.64± 0.01		-
	3	79.47± 0.01		-
70	1	81.52± 0.01	81.47± 0.01	-
	2	81.61± 0.01		-
	3	81.29± 0.01		-
60	1	82.20± 0.01	82.19± 0.01	-
	2	82.28± 0.01		-
	3	82.09± 0.01		-
50	1	83.24± 0.01	83.25± 0.01	-
	2	83.25± 0.01		-
	3	83.28± 0.01		-
40	1	84.39± 0.01	84.89± 0.01	-
	2	84.42± 0.01		-
	3	85.87± 0.01		-
30	1	86.14± 0.01	86.55± 0.01	-
	2	86.13± 0.01		-
	3	87.40± 0.01		-

20	1	89.02± 0.01	89.15± 0.01	-
	2	89.09± 0.01		-
	3	89.35± 0.01		-
15	1	90.90± 0.01	91.03± 0.01	-
	2	90.98± 0.01		-
	3	91.22± 0.01		-
10	1	93.11± 0.01	93.14± 0.01	-
	2	93.08± 0.01		-
	3	93.24± 0.01		-
5	1	96.84± 0.01	96.69± 0.01	-
	2	96.85± 0.01		-
	3	96.38± 0.01		-

Table A-4: Average boiling points of Ethanol-Water mixture at various concentrations and a commercial product

Ethanol (% vol.)	Average boiling point of mixture (°C)	Average boiling point of commercial product (°C)
90	79.58± 0.01	-
70	81.47± 0.01	-
60	82.19± 0.01	-
50	83.25± 0.01	-
40	84.89± 0.01	86.64± 0.01[#]
30	86.55± 0.01	-
20	89.15± 0.01	-
15	91.03± 0.01	-
10	93.14± 0.01	-
5	96.69± 0.01	-

[#] Certified Plumbing Antifreeze, -50 °C

Table A-5: Boiling point of 2-Propanol-Water mixture at various concentrations (3 replicates and their average values)

2-Propanol (% vol.)	Boiling point of mixture (°C)		Average boiling point of mixture (°C)	Observation
90	1	81.04± 0.01	81.04± 0.01	-
	2	81.25± 0.01		-
	3	80.85± 0.01		-
80	1	81.63± 0.01	81.57± 0.01	-
	2	81.69± 0.01		-
	3	81.40± 0.01		-

70	1	81.93± 0.01	81.96± 0.01	-
	2	82.16± 0.01		-
	3	81.80± 0.01		-
60	1	82.47± 0.01	82.35± 0.01	-
	2	82.39± 0.01		-
	3	82.19± 0.01		-
50	1	82.64± 0.01	82.63± 0.01	-
	2	82.70± 0.01		-
	3	82.55± 0.01		-
40	1	83.22± 0.01	83.24± 0.01	-
	2	83.30± 0.01		-
	3	83.20± 0.01		-
30	1	84.21± 0.01	84.13± 0.01	-
	2	84.34± 0.01		-
	3	83.86± 0. 01		-
20	1	86.13± 0.01	85.89± 0.01	-
	2	86.23± 0.01		-
	3	85.33± 0.01		-
10	1	91.49± 0.01	91.63± 0.01	-
	2	91.51± 0.01		-
	3	91.90± 0.01		-
5	1	94.77± 0.01	95.05± 0.01	-
	2	95.14± 0.01		-
	3	95.25± 0.01		-
2	1	98.22± 0.01	98.30± 0.01	-
	2	98.40± 0.01		-
	3	98.30± 0.01		-

Table A-6: Average boiling points of 2-Propanol-Water mixture at various concentrations and a commercial product

2-Propanol (% vol.)	Average boiling point of mixture (°C)	Average boiling point of commercial product (°C)
90	81.04± 0.01	-
80	81.57± 0.01	-
70	81.96± 0.01	82.17± 0.01[§]
60	82.35± 0.01	-
50	82.63± 0.01	-
40	83.24± 0.01	-
30	84.13± 0.01	-
20	85.89± 0.01	-

10	91.63± 0.01	-
5	95.05± 0.01	-
2	98.30± 0.01	-

§ Equate Rubbing Alcohol

Table A-7: Boiling point of Acetone-Water mixtures at various concentrations (3 replicates and their average values)

Acetone (% vol.)	Boiling point of mixture (°C)		Average boiling point of mixture (°C)	Observation
20	1	75.25± 0.01	75.40± 0.01	-
	2	75.50± 0.01		-
	3	75.46± 0.01		-
15	1	79.01± 0.01	79.19± 0.01	-
	2	79.25± 0.01		-
	3	79.32± 0.01		-
10	1	84.22± 0.01	84.47± 0.01	-
	2	84.60± 0.01		-
	3	84.60± 0.01		-
5	1	92.17± 0.01	92.06± 0.01	-
	2	92.09± 0.01		-
	3	91.94± 0.01		-
3	1	95.75± 0.01	95.78± 0.01	-
	2	95.87± 0.01		-
	3	95.74± 0.01		-

Table A-8: Average boiling point of Acetone-Water mixture at various concentrations

Acetone (% vol.)	Average boiling point of mixture (°C)
20	75.40± 0.01
15	79.19± 0.01
10	84.47± 0.01
5	92.06± 0.01
3	95.78± 0.01

Table A-9: Boiling point of Acetic acid-Water mixture at various concentrations (3 replicates and their average values)

Acetic acid (% vol.)	Boiling point of mixture (°C)		Average boiling point of mixture (°C)	Observation
95	1	111.58± 0.01	111.54± 0.01	-

	2	111.51± 0.01		-
	3	111.53± 0.01		-
90	1	108.69± 0.01	108.56± 0.01	-
	2	108.48± 0.01		-
	3	108.51± 0.01		-
80	1	106.11± 0.01	106.05± 0.01	-
	2	106.08± 0.01		-
	3	105.96± 0.01		-
75	1	104.98± 0.01	105.03± 0.01	-
	2	105.03± 0.01		-
	3	105.09± 0.01		-

Table A-10: Average boiling points of Acetic acid-Water mixture at various concentrations and a commercial product

Acetic acid (% vol.)	Average boiling point of mixture (°C)	Average boiling point of commercial product (°C)
95	111.54± 0.01	-
90	108.56± 0.01	-
80	106.05± 0.01	-
75	105.03± 0.01	-
10[Δ]	-	100.5± 0.01

[Δ] Allen's Double Strength Cleaning Vinegar, which contains 10% Acetic acid

Table A-11: Kinematic viscosity of Methanol-Water mixture at various concentrations (3 replicates and their average values)

Methanol (% vol.)	Kinematic viscosity of mixture (cSt)		Average kinematic viscosity of mixture (cSt)	Observation
90	1	0.818± 0.001	0.819± 0.001	-
	2	0.818± 0.001		-
	3	0.820± 0.001		-
80	1	0.991± 0.001	0.992± 0.001	-
	2	0.992± 0.001		-
	3	0.991± 0.001		-
70	1	1.112± 0.001	1.113± 0.001	-
	2	1.114± 0.001		-
	3	1.113± 0.001		-
60	1	1.211± 0.001	1.214± 0.001	-
	2	1.221± 0.001		-
	3	1.211± 0.001		-
50[*]	1	1.236± 0.001	1.231± 0.001	-

	2	1.226± 0.001		-
	3	1.230± 0.001		-
40*	1	1.186± 0.001	1.186± 0.001	-
	2	1.185± 0.001		-
	3	1.185± 0.001		-
30	1	1.094± 0.001	1.095± 0.001	-
	2	1.095± 0.001		-
	3	1.095± 0.001		-
20	1	0.974± 0.001	0.974± 0.001	-
	2	0.974± 0.001		-
	3	0.974± 0.001		-
10	1	0.822± 0.001	0.821± 0.001	-
	2	0.822± 0.001		-
	3	0.821± 0.001		-
5	1	0.755± 0.001	0.755± 0.001	-
	2	0.755± 0.001		-
	3	0.755± 0.001		-

* Additional tested Methanol concentrations

Table A-12: Average kinematic viscosities of Methanol-Water mixture at various concentrations and 2 commercial products

Methanol (% vol.)	Average kinematic viscosity of mixture (cSt)	Average kinematic viscosity of commercial product (cSt)
90	0.819± 0.001	-
80	0.992± 0.001	-
70	1.113± 0.001	-
60	1.214± 0.001	-
50*	1.231± 0.001	1.213†
40*	1.186± 0.001	1.249‡
30	1.095± 0.001	-
20	0.974± 0.001	-
10	0.821± 0.001	-
5	0.755± 0.001	-

* Additional tested Methanol concentrations

† Reflex Windshield Washer Fluid, -49 °C

‡ Certified Windshield Washer Fluid, -35 °C

Table A-13: Kinematic viscosity of Ethanol-Water mixture at various concentrations (3 replicates and their average values)

Ethanol (% vol.)	Kinematic viscosity of mixture (cSt)	Average kinematic viscosity of mixture (cSt)	Observation

90	1	1.431± 0.001	1.429± 0.001	-
	2	1.428± 0.001		-
	3	1.428± 0.001		-
70	1	1.706± 0.001	1.705± 0.001	-
	2	1.704± 0.001		-
	3	1.704± 0.001		-
60	1	1.733± 0.001	1.733± 0.001	-
	2	1.732± 0.001		-
	3	1.733± 0.001		-
50	1	1.688± 0.001	1.688± 0.001	-
	2	1.689± 0.001		-
	3	1.688± 0.001		-
40	1	1.564± 0.001	1.565± 0.001	-
	2	1.565± 0.001		-
	3	1.565± 0.001		-
30	1	1.376± 0.001	1.377± 0.001	-
	2	1.377± 0.001		-
	3	1.377± 0.001		-
20	1	1.134± 0.001	1.134± 0.001	-
	2	1.134± 0.001		-
	3	1.134± 0.001		-
15	1	1.012± 0.001	1.012± 0.001	-
	2	1.012± 0.001		-
	3	1.012± 0.001		-
10	1	0.890± 0.001	0.889± 0.001	-
	2	0.889± 0.001		-
	3	0.888± 0.001		-
5	1	0.780± 0.001	0.780± 0.001	-
	2	0.779± 0.001		-
	3	0.779± 0.001		-

Table A-14: Average kinematic viscosities of Ethanol-Water mixture at various concentrations and a commercial product

Ethanol (% vol.)	Average kinematic viscosity of mixture (cSt)	Average kinematic viscosity of commercial product (cSt)
90	1.429± 0.001	-
70	1.705± 0.001	-
60	1.733± 0.001	-
50	1.688± 0.001	-
40	1.565± 0.001	1.412± 0.001[#]

30	1.377± 0.001	-
20	1.134± 0.001	-
15	1.012± 0.001	-
10	0.889± 0.001	-
5	0.780± 0.001	-

[#] Certified Plumbing Antifreeze, -50 ^{o}C

Table A-15: Kinematic viscosity of 2-Propanol-Water mixtures at various concentrations (3 replicates and their average values)

2-Propanol (% vol.)		Kinematic viscosity of mixture (cSt)	Average kinematic viscosity of mixture (cSt)	Observation
90	1	2.009± 0.001	2.008± 0.001	-
	2	2.007± 0.001		-
	3	2.006± 0.001		-
80	1	2.195± 0.001	2.194± 0.001	-
	2	2.195± 0.001		-
	3	2.193± 0.001		-
70	1	2.252± 0.001	2.250± 0.001	-
	2	2.250± 0.001		-
	3	2.249± 0.001		-
60	1	2.205± 0.001	2.205± 0.001	-
	2	2.206± 0.001		-
	3	2.205± 0.001		-
50	1	2.063± 0.001	2.053± 0.001	-
	2	2.048± 0.001		-
	3	2.048± 0.001		-
40	1	1.846± 0.001	1.836± 0.001	-
	2	1.819± 0.001		-
	3	1.844± 0.001		-
30	1	1.561± 0.001	1.560± 0.001	-
	2	1.560± 0.001		-
	3	1.560± 0.001		-
20	1	1.226± 0.001	1.226± 0.001	-
	2	1.227± 0.001		-
	3	1.225± 0.001		-
10	1	0.925± 0.001	0.923± 0.001	-
	2	0.924± 0.001		-
	3	0.921± 0.001		-
5	1	0.792± 0.001	0.793± 0.001	-
	2	0.794± 0.001		-
	3	0.793± 0.001		-

2	1	0.750± 0.001	0.738± 0.001	-
	2	0.737± 0.001		-
	3	0.728± 0.001		-

Table A-16: Average kinematic viscosities of 2-Propanol-Water mixture at various concentrations and a commercial product

2-Propanol (% vol.)	Average kinematic viscosity of mixture (cSt)	Average kinematic viscosity of commercial product (cSt)
90	2.008± 0.001	-
80	2.194± 0.001	-
70	2.250± 0.001	2.245± 0.001[§]
60	2.205± 0.001	-
50	2.053± 0.001	-
40	1.836± 0.001	-
30	1.560± 0.001	-
20	1.226± 0.001	-
10	0.923± 0.001	-
5	0.793± 0.001	-
2	0.738± 0.001	-

[§] Equate Rubbing Alcohol

Table A-17: Kinematic viscosity of Acetone-Water mixture at various concentrations (3 replicates and their average values)

Acetone (% vol.)	Kinematic viscosity of mixture (cSt)		Average kinematic viscosity of mixture (cSt)	Observation
20	1	0.907± 0.001	0.908± 0.001	-
	2	0.907± 0.001		-
	3	0.910± 0.001		-
15	1	0.858± 0.001	0.855± 0.001	-
	2	0.854± 0.001		-
	3	0.854± 0.001		-
10	1	0.797± 0.001	0.797± 0.001	-
	2	0.797± 0.001		-
	3	0.797± 0.001		-
5	1	0.742± 0.001	0.740± 0.001	-
	2	0.739± 0.001		-
	3	0.739± 0.001		-
3	1	0.716± 0.001	0.716± 0.001	-
	2	0.716± 0.001		-
	3	0.716± 0.001		-

Table A-18: Average kinematic viscosity of Acetone-Water mixture at various concentrations

Acetone (% vol.)	Average kinematic viscosity of mixture (cSt)
20	0.908± 0.001
15	0.855± 0.001
10	0.797± 0.001
5	0.740± 0.001
3	0.716± 0.001

Table A-19: Kinematic viscosity of Acetic acid-Water mixture at various concentrations (3 replicates and their average values)

Acetic acid (% vol.)	Kinematic Viscosity of mixture (cSt)		Average kinematic viscosity of mixture (cSt)	Observation
95	1	1.251± 0.001	1.254± 0.001	-
	2	1.261± 0.001		-
	3	1.250± 0.001		-
90	1	1.477± 0.001	1.465± 0.001	-
	2	1.458± 0.001		-
	3	1.460± 0.001		-
80	1	1.638± 0.001	1.635± 0.001	-
	2	1.636± 0.001		-
	3	1.631± 0.001		-
75	1	1.624± 0.001	1.623± 0.001	-
	2	1.624± 0.001		-
	3	1.622± 0.001		-

Table A-20: Average kinematic viscosities of Acetic acid-Water mixture at various concentrations and a commercial product

Acetic acid (% vol.)	Average kinematic viscosity of mixture (cSt)	Average kinematic viscosity of commercial product (cSt)
95	1.254± 0.001	-
90	1.465± 0.001	-
80	1.635± 0.001	-
75	1.623± 0.001	-
10[Δ]	-	0.807± 0.001

[Δ] Allen's Double Strength Cleaning Vinegar, which contains 10% Acetic acid

Table A-21: Open-cup flash point of Methanol-Water mixture at various concentrations (3 replicates and their average values)

Methanol (% vol.)	Flash point of mixture (°C)		Average flash point of mixture (°C)	Observation
90	1	15.0±1	15.7±1	Flash points = Fire points
	2	15.5±1		
	3	16.5±1		
80	1	17.0±1	17.6±1	
	2	18.0±1		
	3	17.8±1		
70	1	20.5±1	20.4±1	
	2	20.2±1		
	3	20.5±1		
60	1	22.2±1	22.4±1	
	2	22.5±1		
	3	22.5±1		
50*	1	26.5±1	26.1±1	
	2	25.8±1		
	3	26.0±1		
40*	1	35.0±1	35.2±1	
	2	36.0±1		
	3	34.5±1		
30	1	39.0±1	42.0±1	Both flash and fire points were observed
	2	43.0±1		
	3	44.0±1		
20	1	56.5±1	57.0±1	
	2	57.0±1		
	3	57.5±1		
10	1	-	-	No flash and fire point were observed up to 60 °C
	2	-		
	3	-		
5	1	-	-	
	2	-		
	3	-		

**Additional tested Methanol concentrations.

Table A-22: Comparison of experimental open-cup flash points of Methanol-Water mixture with theoretical closed-cup values and 2 commercial products

Methanol (% vol.)	Average flash point of mixture (°C)	Theoretical flash point (°C)[¶]	Average flash point of commercial product (°C)
90	15.7±1	13	-
80	17.6±1	15	-
70	20.4±1	19	-
60	22.4±1	22	-
50[*]	26.1±1	26	26.7±1[†]
40[*]	35.2±1	27	27.5±1[‡]
30	42.0±1	39	-
20	57.0±1	48	-
10	-	58	-
5	-	-	-

[*] Additional tested Methanol concentrations
[¶] Taken from project Phase 1 report [1]
[†] Reflex Windshield Washer Fluid, -49 °C
[‡] Certified Windshield Washer Fluid, -35 °C

Table A-23: Open-cup fire point of Methanol-Water mixture at various concentrations (3 replicates and their average values)

Methanol (% vol.)	Fire point of mixture (°C)		Average fire point of mixture (°C)	Observation
90	1	15.0±1	15.7±1	Flash points = Fire points
	2	15.5±1		
	3	16.5±1		
80	1	17.0±1	17.6±1	
	2	18.0±1		
	3	17.8±1		
70	1	20.5±1	20.4±1	
	2	20.2±1		
	3	20.5±1		
60	1	22.2±1	22.4±1	
	2	22.5±1		
	3	22.5±1		
50[*]	1	26.5±1	26.1±1	Flash points = Fire points
	2	25.8±1		
	3	26.0±1		
40[*]	1	35.0±1	35.2±1	

	2	36.0±1		
	3	34.5±1		
30	1	42.0±1	44.7±1	Both flash and fire points were observed
	2	46.0±1		
	3	46.0±1		
20	1	64.0±1	64.2±1	
	2	65.5±1		
	3	63.0±1		
10	1	-	-	No flash and fire points were observed up to 60 °C
	2	-		
	3	-		
5	1	-	-	
	2	-		
	3	-		

* Additional tested Methanol concentrations

Table A-24: Comparison of experimental open-cup fire points of Methanol-Water mixture with theoretical closed-cup values, and 2 commercial products

Methanol (% vol.)	Average fire point of mixture (°C)	Theoretical fire point (°C)¶	Average fire point of commercial product (°C)
90	15.7±1	21.8	-
80	17.6±1	23.9	-
70	20.4±1	26.1	-
60	22.4±1	28.6	-
50*	26.1±1	31.1	28.0±1†
40*	35.2±1	34.4	27.0±1‡
30	44.7±1	37.7	-
20	64.2±1	46.2	-
10	-	54.6	-
5	-	69.3	-

* Additional tested Methanol concentrations
¶ Taken from project Phase 1 report [1]
† Reflex Windshield Washer Fluid, -49 °C
‡ Certified Windshield Washer Fluid, -35 °C

Table A-25: Open-cup flash point of Ethanol-Water mixture at various concentrations (3 replicates and their average values)

Ethanol (% vol.)	Flash point of mixture (°C)	Average flash point of mixture (°C)	Observation

90	1	13.5±1	14.0±1	Flash points = Fire points
	2	14.0±1		
	3	14.5±1		
70	1	19.5±1	19.5±1	
	2	20.0±1		
	3	19.0±1		
60	1	21.5±1	21.0±1	Both Flash and fire points were observed
	2	21.5±1		
	3	20.0±1		
50	1	22.0±1	22.5±1	
	2	23.5±1		
	3	22.0±1		
40	1	29.0±1	29.6±1	
	2	30.5±1		
	3	29.5±1		
30	1	33.5±1	34.6±1	
	2	35.5±1		
	3	35.0±1		
20	1	45.0±1	45.8±1	
	2	46.0±1		
	3	46.5±1		
15	1	52.5±1	52.5±1	
	2	52.0±1		
	3	53.0±1		
10	1	57.5±1	58.2±1	
	2	59.0±1		
	3	58.0±1		
5	1	-	-	No flash and fire points were observed up to 60 °C
	2	-		

Table A-26: Comparison of experimental open-cup flash points of Ethanol-Water mixture with theoretical closed-cup values, and a commercial product

Ethanol (% vol.)	Average flash point of mixture (°C)	Theoretical flash point (°C)¶	Average flash point of commercial product (°C)
90	14.0±1	17	-
70	19.5±1	20	-

60	21.0±1	21	-
50	22.5±1	22	-
40	29.6±1	24	32.2±1[#]
30	34.6±1	26	-
20	45.8±1	29	-
15	52.5±1	36	-
10	58.2±1	49	-
5	-	62	-

[#] Certified Plumbing Antifreeze, -50 °C
[¶] Taken from project Phase 1 report [1]

Table A-27: Open-cup fire point of Ethanol-Water mixture at various concentrations (3 replicates and their average values)

Ethanol (% vol.)	Fire point of mixture (°C)		Average fire point of mixture (°C)	Observation
90	1	13.5±1	14.0±1	Flash points = Fire points
	2	14.0±1		
	3	14.5±1		
70	1	19.5±1	19.5±1	
	2	20.0±1		
	3	19.0±1		
60	1	25.0±1	24.7±1	Both Flash and fire points were observed
	2	25.0±1		
	3	24.0±1		
50	1	27.0±1	27.8±1	
	2	28.5±1		
	3	28.0±1		
40	1	35.0±1	35.2±1	
	2	36.0±1		
	3	34.5±1		
30	1	44.0±1	45.8±1	
	2	47.0±1		
	3	46.5±1		
20	1	58.5±1	59.5±1	
	2	60.0±1		
	3	60.0±1		
15	1	63.0±1	64.0±1	
	2	64.5±1		

	3	64.5±1		
10	1	67.5±1	67.8±1	Both Flash and fire points were observed
	2	68.0±1		
	3	68.0±1		
5	1	-	-	No flash and fire points were observed up to 60 °C
	2	-		
	3	-		

Table A-28: Comparison of experimental open-cup fire points of Ethanol-Water mixture with theoretical closed-cup values, and a commercial product

Ethanol (% vol.)	Average fire point of mixture (°C)	Theoretical fire point (°C)¶	Average fire point of commercial product (°C)
90	14.0±1	25.5	-
70	19.5±1	30	-
60	24.7±1	31.5	-
50	27.8±1	33.5	-
40	35.2±1	36	39.8±1#
30	45.8±1	40	-
20	59.5±1	46.5	-
15	64.0±1	52.25	-
10	67.8±1	58	-
5	-	-	-

Certified Plumbing Antifreeze, -50 °C

¶ Taken from project Phase 1 report [1]

Table A-29: Open-cup flash point of 2-Propanol-Water mixture at various concentrations (3 replicates and their average values)

2-Propanol (% vol.)	Flash point of mixture (°C)		Average flash point of mixture (°C)	Observation
90	1	15.5±1	15.3±1	Flash points = Fire points
	2	15.5±1		
	3	15.0±1		
80	1	18.5±1	17.6±1	
	2	17.5±1		
	3	17.0±1		
70	1	19.0±1	19.0±1	Both flash and fire points were observed
	2	19.5±1		
	3	18.5±1		

60	1	22.0±1	21.0±1	Both flash and fire points were observed
	2	20.5±1		
	3	20.5±1		
50	1	21.0±1	21.6±1	
	2	22.0±1		
	3	22.0±1		
40	1	24.5±1	23.3±1	
	2	23.5±1		
	3	23.5±1		
30	1	31.0±1	30.3±1	
	2	31.0±1		
	3	29.0±1		
20	1	36.0±1	35.6±1	
	2	36.0±1		
	3	35.0±1		
10	1	54.0±1	54.3±1	
	2	54.0±1		
	3	55.0±1		
5	1	-	-	No flash and fire points were observed up to 60 °C
	2	-		
	3	-		
2	1	-	-	
	2	-		
	3	-		

Table A-30: Comparison of experimental open-cup flash points of 2-Propanol-Water mixture with theoretical closed-cup values, and a commercial product

2-Propanol (% vol.)	Average flash point of mixture (°C)	Theoretical flash point (°C)[¶]	Average flash point of commercial product (°C)
90	15.3±1	18	-
80	17.6±1	19	-
70	19.0±1	21	19.2±1[§]
60	21.0±1	21	-
50	21.6±1	21	-
40	23.3±1	23	-
30	30.3±1	25	-
20	35.6±1	30	-

10	54.3±1	41	-
5	-	50	-
2	-	65	-

§ Equate Rubbing Alcohol

¶ Taken from project Phase 1 report [1]

Table A-31: Open-cup fire point of 2-Propanol-Water mixtures at various concentrations (3 replicates and their average values)

2-Propanol (% vol.)	Fire point of mixture (°C)		Average fire point of mixture (°C)	Observation
90	1	15.5±1	15.3±1	Flash points = Fire points
	2	15.5±1		
	3	15.0±1		
80	1	18.5±1	17.6±1	
	2	17.5±1		
	3	17.0±1		
70	1	22.0±1	21.2±1	Both flash and fire points were observed
	2	21.0±1		
	3	20.5±1		
60	1	25.0±1	23.5±1	
	2	22.0±1		
	3	23.5±1		
50	1	25.5.0±1	25.5±1	
	2	26.0±1		
	3	25.0±1		
40	1	34.0±1	32.6±1	
	2	32.0±1		
	3	32.0±1		
30	1	34.0±1	34.3±1	
	2	35.0±1		
	3	34.0±1		
20	1	50.0±1	49.2±1	
	2	49.5±1		
	3	48.0±1		
10	1	68.5±1	68.8±1	
	2	69.0±1		
	3	-		
5	1	-	-	
	2	-		

	3	-		No flash and fire points were observed up to 60 °C
2	1	-	-	
	2	-		
	3	-		

Table A-32: Comparison of experimental open-cup fire points of 2-Propanol-Water mixture with theoretical closed-cup values and a commercial product

2-Propanol (% vol.)	Average fire point of mixture (°C)	Theoretical fire point (°C)¶	Average fire point of commercial product (°C)
90	15.3±1	28	-
80	17.6±1	29	-
70	21.2±1	31	20.2§
60	23.5±1	31	-
50	25.5±1	31	-
40	32.6±1	33	-
30	34.3±1	35	-
20	49.2±1	40	-
10	68.8±1	51	-
5	-	60	-
2	-	75	-

§ Equate Rubbing Alcohol

¶ Taken from project Phase 1 report [1]

Table A-33: Open-cup flash point of Acetone-Water mixture at various concentrations (3 replicates and their average values)

Acetone (% vol.)	Flash point of mixture (°C)		Average flash point of mixture (°C)	Observation
20	1	10.5±1	10.7±1	Both flash and fire points were observed
	2	10.5±1		
	3	11.0±1		
15	1	14.5±1	15.2±1	
	2	16.0±1		
	3	15.0±1		
10	1	27.0±1	26.5±1	
	2	25.0±1		
	3	27.5±1		
5	1	49.0±1	50.7±1	
	2	52.0±1		

	3	51.0±1		
3	1	-	-	No flash and fire points were observed up to 60 °C
	2	-		
	3	-		

Table A-34: Comparison of experimental open-cup flash points of Acetone-Water mixture with theoretical closed-cup values

Acetone (% vol.)	Average flash point of mixture (°C)	Theoretical flash point (°C)¶
20	10.7±1	3
15	15.2±1	8
10	26.5±1	16
5	50.7±1	29
3	-	36

¶ Taken from project Phase 1 report [1]

Table A-35: Open-cup fire point of Acetone-Water mixture at various concentrations (3 replicates and their average values)

Acetone (% vol.)	Fire point of mixture (°C)		Average fire point of mixture (°C)	Observation
20	1	18.5±1	18.2±1	Both flash and fire points were observed
	2	17.0±1		
	3	19.0±1		
15	1	26.0±1	26.5±1	
	2	26.5±1		
	3	27.0±1		
10	1	32.0±1	32.2±1	
	2	31.5±1		
	3	33.0±1		
5	1	53.0±1	53.8±1	
	2	54.0±1		
	3	54.5±1		
3	1	-	-	No flash and fire points were observed up to 60 °C
	2	-		
	3	-		

Table A-36: Comparison of experimental open-cup fire points of Acetone-Water mixture with theoretical closed-cup values

Acetone (% vol.)	Average fire point of mixture (°C)	Theoretical fire point (°C)¶
20	18.2±1	13
15	26.5±1	19.5
10	32.2±1	26
5	53.8±1	39.5
3	-	-

¶ Taken from project Phase 1 report [1]

Table A-37: Open-cup flash point of Acetic acid-Water mixture at various concentrations (3 replicates and their average values)

Acetic acid (% vol.)	Flash point of mixture (°C)		Average flash point of mixture (°C)	Observation
95	1	53.0±1	52.7±1	Both flash and fire points were observed
	2	53.0±1		
	3	52.0±1		
90	1	63.0±1	61.8±1	Only flash points were observed
	2	60.5±1		
	3	62.0±1		
80	1	81.5±1	78.2±1	
	2	76.0±1		
	3	77.0±1		
75	1	-	-	No flash and fire points were observed up to 85 °C
	2	-		
	3	-		

Table A-38: Comparison of experimental open-cup flash points of Acetic acid-Water mixture with theoretical closed-cup values

Acetic acid (% vol.)	Average flash point of mixture (°C)	Theoretical flash point (°C)¶
95	52.7±1	51
90	61.8±1	45
80	78.2±1	59
75	-	-

¶ Taken from project Phase 1 report [1]

Table A-39: Open-cup fire point of Acetic acid-Water mixture at various concentrations (3 replicates and their average values)

Acetic Acid (% vol.)	Fire point of mixture (°C)		Average fire point of mixture (°C)	Observation
95	1	75.3±1	75.4±1	Both flash and fire points were observed
	2	76.0±1		
	3	75.0±1		
90	1	-	-	No fire points were observed
	2	-		
	3	-		
80	1	-	-	
	2	-		
	3	-		
75	1	-	-	No flash and fire points were observed up to 85 °C
	2	-		
	3	-		

Table A-40: Comparison of experimental open-cup fire points of Acetic acid-Water mixture with theoretical closed-cup values

Acetic acid (% vol.)	Average fire point of mixture (°C)	Theoretical fire point (°C)¶
95	75.4±1	54.5
90	-	61
80	-	69
75	-	74

¶ Taken from project Phase 1 report [1]

Appendix B – Sample Calculations for Permeability, Diffusivity and Solubility

The following calculations are done for a PPO membrane with the following conditions/properties summarized in Table B-1.

Table B-1: Summary of inputs for permeability, diffusivity and solubility calculations

Parameter	Symbol	Value	Units
Pressure rise	dp/dt	0.000906	Torr/s
Pressure	Δp	1650	Torr
Volume	V	0.000085	m^3
Membrane Area	A	0.0114	m^2
Temperature	T	303	K
Time Lag	Θ	373.5	s
Gas Constant	R	8.3145	J/mol-K
Molar Volume	v	0.00024	cm^3 (STP)/mol
Membrane Thickness	L	0.00008	m

$$\frac{dp}{dt} = 0.000906255\frac{Torr}{s} \times \frac{101325}{760}\frac{Pa}{Torr} = 0.120824\frac{Pa}{s}$$

$$p = 1650\,Torr\ \times \frac{101325}{760}\frac{Pa}{Torr} = 219981.9\,Pa$$

$$Molar\ Flow\ (Q) = \frac{\left(\frac{dp}{dt}\right)V}{RT} = \frac{(0.120824\frac{Pa}{s})(0.000085\,m)}{(8.3145\frac{J}{mol\ K})(303\,K)} = 4.0768 \times 10^{-9}\frac{mol}{s}$$

$$Molar\ Flux\ (N) = \frac{4.0768 \times 10^{-9}\frac{mol}{s}}{0.0114\,m^2} = 3.576 \times 10^{-9}\frac{mol}{s\,m^2}$$

$$Permeability\ (P) = \frac{Molar\ Flux\ (N) \times Pressure(\Delta p)}{Membrane\ Thickness\ (L)} = \frac{3.576 \times 10^{-9}\frac{mol}{s\,m^2}}{0.00008\,m}$$

$$= 1.30\ \times 10^{-15}\frac{mol}{s\,m^2 Pa}$$

$$\frac{1.30\ \times 10^{-15}\frac{mol}{s\,m^2 Pa}}{3.35 \times 10^{-16}\frac{SI\ Units}{Barrer}} = \mathbf{3.88\ Barrer}$$

$$Diffusivity\ (D) = \frac{L^2}{6\theta} = \frac{0.00008m}{(6)(373.5)} = \mathbf{2.855 \times 10^{-12}\,\frac{m^2}{s}}$$

$$Solubility\ (S) = \frac{P}{D} = \frac{\left(3.88\ Barrer\ \times \frac{10^{10}\,\frac{cm^3(STP)cm}{s\ cm^2 cmHg}}{Barrer}\right)}{\left(2.855 \times 10^{-12}\,\frac{m^2}{s} \times \frac{100^2 cm^2}{1\ m^2}\right)} = \mathbf{1.36 \times 10^{-2}\,\frac{cm^3}{cm^3 cmHg}}$$